

Spectroscopy of the Intermediate States of the Solid State Polymerization Reaction in Diacetylene Crystals

Hans Sixl

Physikalisches Institut, Teil 3, Universität Stuttgart

Pfaffenwaldring 57, D-7000 Stuttgart 80, FRG

This contribution gives a review of recent spectroscopic investigations concerning the photophysical and photochemical primary and secondary processes of the solid state polymerization reaction in diacetylene single crystals. It will be shown, that diacetylenes are an unique model system for the study of the reaction mechanism of a solid state chemical reaction which is characterized by a variety of reaction intermediates. The polymerization reaction in these crystals is of special importance, due to the resulting polymer single crystals, which exhibit extraordinary anisotropic physical properties.

ESR (electron spin resonance) and optical absorption spectroscopy at low temperatures were used to analyse the individual reaction steps of the optical and thermal polymerization reactions and their kinetics. The reaction steps are

*the photoinitiation,
the chain propagation and
chain termination reactions.*

It is possible to exactly identify and characterize the radical species and chain structures of the reaction intermediates, which are determined by their different reactive or unreactive chain ends. The reactive intermediates are best described by diradical (DR), asymmetric carbene (AC) and dicarbene (DC) oligomer molecules of different lengths. The respective singlet ($S = 0$), triplet ($S = 1$) or quintet ($S = 2$) states and their roles in the polymerization process are investigated in detail by solid state spectroscopy. A one-dimensional electron gas model is successfully applied to the optical absorption series of the DR and AC intermediates as well as on the different stable oligomer SO molecules obtained after final chain termination reactions.

1 Introduction	51
1.1 Polymer Single Crystals	51
1.2 Solid-State Polymerization	51
1.3 Spectroscopic Investigations	54
1.4 Reaction Mechanism	55
2 The Intermediates of the Low Temperature Photoreaction	57
2.1 Optical Absorption Spectra	57
2.2 ESR Absorption Spectra	61
2.3 Correlation of the Photoproducts	66
2.4 The Individual Steps of the Low Temperature Photopolymerization Reactions	68
2.5 Reaction Scheme of the Low Temperature Photoreactions	72
3 Thermal Reactions of the Low Temperature Photoproducts	72
3.1 Optical Absorption Spectra	72
3.2 ESR-Spectra	73
3.3 The Thermal Reaction Steps	77

4 Kinetics	79
4.1 Rate Equations	79
4.2 Chain Lengths Distribution	80
5 Primary Processes	82
5.1 Dimer Initiation	82
5.2 Stability and Reactivity	84
6 Conclusions.	87
7 References	88

1 Introduction

1.1 Polymer Single Crystals

Applying conventional procedures polymerization reactions are generally performed in the fluid phase¹⁾. As a rule the macromolecules produced in this reaction form either glassy or chainfolded microcrystalline polymer. The original extreme anisotropy of the individual "one-dimensional" polymer filaments is lost due to the arbitrary orientations of the polymer segments in such materials. Therefore in general the mechanical and optical properties of typical polymer foils are completely isotropic. The crystallization of a polymer solution or melt fails to produce macroscopic polymer single crystals, due to the enormous length and flexibility of the polymer chains²⁾.

The progress of spectroscopic research concerning the electronic properties of conventional organic polymers has been severely hindered by their gross structural inhomogeneities. Typical microscopic polymer crystals distributed in bulk polycrystalline polymers grow from solution (e.g. polyethylene²⁾) have chain axis dimensions of about 100 Å. Moreover defects such as dislocations, chain kinks and cross-linking restrict the lengths of the quasi one-dimensional chain Sections^{3,4)}. The physical properties of polymeric materials are strongly dependent on the defect structures. The isotropic distribution of the crystallites in bulky polymers excludes the investigation of the intrinsic anisotropic properties of the individual polymer filaments. Detailed analysis has not been possible with spectroscopic methods, such as ESR- or X-ray structure analysis which are most powerful with single crystalline samples. For all these reasons there has been considerable interest in macroscopic polymer single crystals.

Nearly perfect large-dimension polymer single crystals were only recently successfully synthesized from monomers by solid state polymerization⁵⁻¹⁴⁾. This method has been most successful in the preparation of polydiacetylene single crystals. The reaction mechanisms of this remarkable solid state reaction will be discussed in this contribution. A second method (which yields less perfect polymer crystals or only ordered polymer filaments) involves nearly simultaneous crystallization and polymerization of monomer molecules at liquid-solid or gas-solid interfaces^{15,16)}. This method has been most successful in the preparation of polysulphur nitride (SN)_x "crystals", which in contrast to the large band-gap semiconducting polydiacetylene crystals¹⁷⁻²¹⁾ is a polymer metal with superconductive properties below about 0.3 K²²⁾. The interest of both chemists and physicists in polymer crystals is based on the extraordinary anisotropic optical and electrical properties expected from the regular periodic arrangement of the linear filaments in the polymer single crystals.

1.2 Solid-State Polymerization

In contrast to conventional methods the polymerization of diacetylenes proceeds within the original monomer crystal which can be grown from solution. In ideal cases, for example TS-6 [bis(p-toluene sulphonate) ester of 2,4hexadiyne-1,6-diol], the polymerization reaction transforms a monomer molecular crystal to a polymer

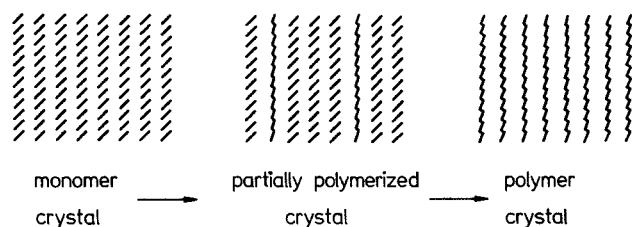


Fig. 1. Schematic representation of the solid state polymerization reaction at room temperature. The partially polymerized monomer crystal contains long polymer filaments

crystals with nearly the same dimensions and similar structural perfection⁵⁻¹⁴). The reaction is shown schematically in Fig. 1. Mostly the reaction is initiated photochemically [by highly energetic UV, X-ray, or γ -ray quanta ($h\nu$)] or thermally [by heat (kT), i.e., by lattice or molecular vibrations]. The polymer filaments then grow in the monomer stacking plane (see Fig. 2). In the ideal case the polymer enters the polymerizing lattice as a solid solution over the entire monomer-to-polymer conversion range. In this way phase separation between monomer and polymer with the associated shear and volume strains are avoided^{23,24}). Brillouin scattering experiments²⁴), scanning electron microscopy²⁵), gel permeation chromatography²⁶), optical spectroscopy²⁷) and laser holography²⁸) confirm that extremely long chains of about 100 to 1000 monomer units are formed within the partially polymerized monomer crystals.

As for most solid state reactions the "topochemical principle"²⁹⁻³¹) is valid in this specific polymerization reaction. It may be formulated as follows: The reactions in solids are performed with a minimum in the atomic and molecular motion (principle of least motion). Therefore, the occurrence of a chemical reaction and the stereo-

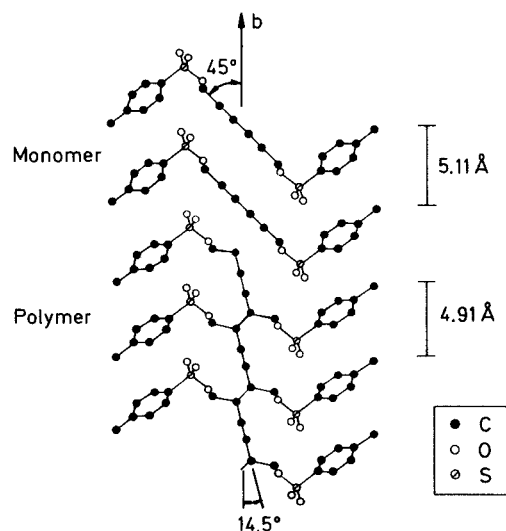
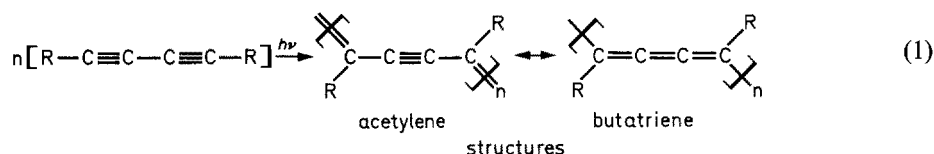


Fig. 2. Comparison of the atomic positions in the monomer and in the polymer crystal as deduced from X-ray data³⁶)

chemistry of the reaction products are determined by the monomer crystal structure and the positions of the reactive groups within individual molecules. Applying these principles it is possible to synthesize highly stereoregular extended-chain polymers, which are impossible to be prepared by alternative means. The conception, therefore, is to produce crystals in which the monomers, each with their two potential reactive centres, are oriented so that they can rotate in place to link up with their neighbours. An optimal arrangement of the monomer molecules is obtained by an appropriate choice of their substituents R. The best conditions are obtained in the absence of any linear displacement of the molecular centres. In other cases a change in the lattice parameters associated with mechanical stress diminishes the reactivity. Large stress due to inhomogeneous polymerization may lead to the destruction of the crystals as for example in the case of distyrylpyrazine^{32,33} and other $2\pi + 2\pi$ photocyclizations.

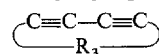
The polymerization of the diacetylene crystals is usually described by the following reaction equation



Fully conjugated and fully chain-aligned polymer single crystals with planar polymer backbone³⁴) are obtained, which may have the alternative acetylene (ynene) or butatriene structures of Eq. (1). From our experiment we know that the acetylene structure is dominant in the polymer molecules. Up to now the best investigated diacetylene crystals are the TS-6 monomer crystals and the corresponding polymer crystals (poly TS-6). The substituents R and the notation of further diacetylene crystals discussed below are listed in Table 1.

The atomic positions and the lattice parameters of the monomer and polymer crystals have been determined by X-ray analysis³⁴⁻³⁸). Fig. 2 shows the projection of the monomer and polymer molecules on the plane of the polymer backbone. The positions of the substituents $R = \text{CH}_2\text{SO}_3\text{C}_6\text{H}_4\text{CH}_3$ are only slightly changed, however the central diacetylene unit $-\text{C}\equiv\text{C}-\text{C}\equiv\text{C}-$ is rotated within the plane of the backbone by an angle of about 30° .

Table 1. Some examples of diacetylene crystals of the structure $R-C\equiv C-C\equiv C-R$, $R_1-C\equiv C-C\equiv C-R_2$ and



Notations	Substituents
TS-6	R: $-\text{CH}_2\text{OSO}_2\text{C}_6\text{H}_4\text{CH}_3$
TS-12	R: $-(\text{CH}_2)_4\text{OSO}_2\text{C}_6\text{H}_4\text{CH}_3$
FBS-6	R: $-\text{CH}_2\text{OSO}_2\text{C}_6\text{H}_4\text{F}$
TCDU	R: $-(\text{CH}_2)_4\text{OCONHC}_6\text{H}_5$
TCDA	$R_1: -(\text{CH}_2)_9\text{CH}_3$, $R_2: -(\text{CH}_2)_8\text{COOH}$
BPG	$R_3: -\text{OCO}(\text{CH}_2)_3\text{OCO}-$

1.3 Spectroscopic Investigations

The polydiacetylene crystals have striking spectroscopic properties, which have been utilized in studies of their electrical¹⁷⁻²¹⁾, structural³⁴⁻³⁸⁾ and optical³⁹⁻⁴³⁾ behavior. These properties are in contrast to those of the monomer crystals, which show the characteristic features of molecular single crystals. As a consequence of the construction of a fully chain aligned polymer structure the mechanical and optical properties of the diacetylene crystals change dramatically during the phase transition from monomer to polymer. This effect is demonstrated in Fig. 3 by example of the optical absorption spectrum of a typical diacetylene crystal at room temperature⁴⁴⁾. The clear and fully transparent monomer crystals (with absorptions in the ultraviolet spectral region, starting at about 300 nm, viz. $33,000\text{ cm}^{-1}$) become coloured with increasing polymerization from pink to deep red and finally obtain a metallic lustre in the fully polymerized state.

A direct measure of the optical absorption coefficient α is the optical density OD defined by $OD = \log I_0/I = 0,434\alpha d$ (I_0 and I are the incident and the transmitted light intensities and d is the thickness of the crystal). Weak polymer absorption in the range from 600 to 400 nm is present in the original monomer crystals due to weak thermal polymerization reactions. The absorption of the linear polymer molecules (which are homogeneously distributed within the partially polymerized monomer diacetylene crystals) increase during UV-irradiation at room temperature due to photopolymerization reactions. In contrast to the monomer absorption, the polymer

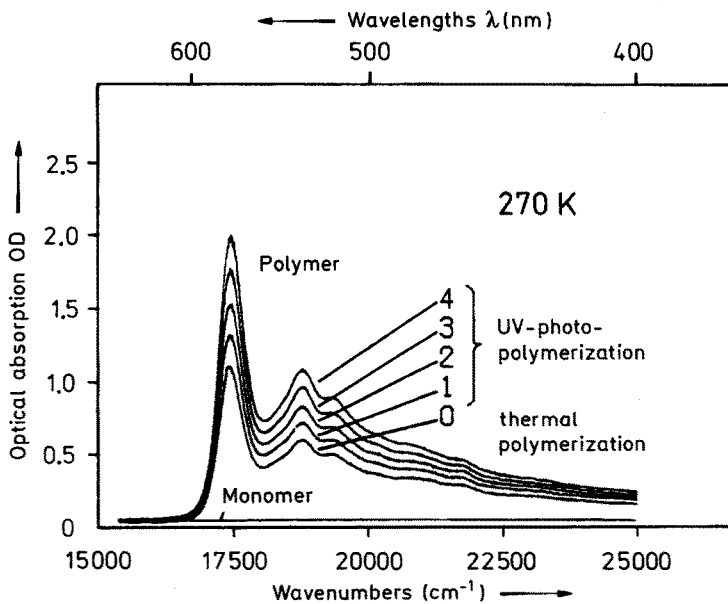


Fig. 3. Optical absorption spectra of a diacetylene crystal (TS-6) at about room temperature. The optical density is proportional to the absorption coefficient. The absorption in the visible spectral region is due to the polymer filaments. UV photopolymerization has been performed in steps using the same photon numbers, respectively

absorption is extremely anisotropic with $\alpha_{\parallel}:\alpha_{\perp} \approx 10^4$ ^{41,43}). All optical absorption spectra presented in this review are polarized with electric field vector E of the incident light parallel to the chain direction $b(E\parallel b)$, since for $E \perp b$ no absorption of the polymer chains is observed under the prevailing experimental conditions.

At the ends of the polymer chains and at the ends of the short oligomer units (see for example the trimer molecule of Table 1) a bond defect structure is expected. For the acetylene structure of the polymer chain this is a carbene $-\dot{C}-$ with two free valence electrons and in the case of the butatriene structure this is a *radical carbon* atom $-\dot{C}=\dot{C}=\dot{C}-$ with one free valence electron. In both cases there is a reactive chain end, which allows reaction of the chain with the neighbouring monomer molecules. These reactive structures and a possible nonreactive structure are listed in Table 1 as examples of the trimer molecules.

Structure and kinetics of the radical ends (with electron spin $S = 1/2$) and of the carbene ends (with $S = 1$) are in principle investigated most effectively by the methods of electron spin resonance (ESR) and by electron nuclear double resonance (ENDOR). Information on the lengths and structures of the butatriene or acetylene short oligomer molecules should be obtained from optical absorption spectra, completely analogous to that for the well known linear dye molecules of different lengths described by the theory of Kuhn^{45,46}). Both methods are highly suitable for investigating the electronic structure of the reaction intermediates and the kinetics of the solid state polymerization reaction. Due to the fast polymerization reaction at room temperature the spectroscopic methods were mainly restricted to the investigation of the polymer species. Through these studies it was, in fact, possible to detect triplet carbenes and doublet radical species at low concentrations⁴⁷⁻⁵⁰). However, it proved impossible to spectroscopically detect short dimer-, trimer-, . . . and oligomer-intermediates at room temperature. This is due to their extremely short lifetimes which, as we will see later, range in the nanosecond to microsecond time scale (see for example the experiments of Niederwald et al.^{51,52}).

1.4 Reaction Mechanism

For a detailed investigation of the individual steps of the polymerization reaction, including the different intermediates of both the initiation reaction (formation of the dimer) as well as the subsequent addition polymerization reactions (formation of the trimer, tetramer, . . .), it is necessary to slow down or even stop the reaction by cooling the crystals. Consequently the concept of the following spectroscopic investigations is to photochemically initiate the polymerization reaction at extremely low temperatures (10 K) and to investigate the structure and kinetics of the intermediates obtained in subsequent photochemical or thermal reaction steps. The first low temperature experiments have been performed by Hori and Kispert using X-irradiation^{53,54}), and by Bubeck et al.^{55,56}) and Hersel et al.^{57,58}) using UV-irradiation.




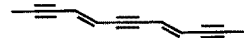
The reaction mechanisms of this extraordinary solid state reaction has strongly attracted the interest of the polymer chemists from the very beginning. Valuable information on several aspects of the thermal polymerization reaction mechanisms, have been obtained from X-ray structural and physico-chemical investigations, discussed by Wegner^{59,60}), Baughman^{10,11}) and Chance⁶¹). However, the identifi-

cation and detailed characterization of the individual reaction intermediates and their kinetics has been obtained only by spectroscopic investigations at low temperatures^{55-58,62-69}) as discussed in this review.

From spectroscopic data, presented in the following, we conclude that the mechanism of polymerization is described by three series of intermediate states differing by the number of reactive radical or carbene chain ends: these are the *diradicals* "DR", the *dicarbenes* "DC", and the *asymmetric carbenes* "AC". Via a final chain termination reaction an additional series of reaction products is obtained. These are the *stable oligomers* "SO" with two unreactive chain ends. The schematic structures of the DR, DC, AC, and SO molecules are shown by example of the trimer in Table 2. The lengths of the dimer-, trimer-, tetramer- . . . units are characterized by the numbers $n = 2, 3, 4, \dots$ of the respective monomer molecules. The symbols and the schematic structures as well as the notation of the optical and the ESR absorption lines, are summarized in Table 2.

In all experiments described in this work only extremely low concentrations of intermediates are considered. This is due to our interest which is primarily focussed on the most important initial steps of the polymerization reaction, which are characteristic of the overall polymerization reaction mechanism. Consequently only low final polymer conversion is expected and, therefore, complications arising from the interaction between the intermediate oligomer states can be neglected. It will be shown that the low temperature conventional optical absorption and ESR spectroscopy are powerful spectroscopic methods which yield a wealth of information concerning structural and dynamical aspects of the intermediate states in the photopolymerization reaction of diacetylene crystals. Therefore, this contribution will center on the photochemical and photophysical primary and secondary processes of this

Table 2. Symbols, spin multiplicities, structures and notations. The simplified structures of the reaction intermediates and of the final stable products are shown schematically by example of the trimer molecule

Symbols	Structures	Notations		
		Chains	Optics	ESR
Spin S	Simplified structures	Chains	Optics	ESR
—DR— diradicals $S = 0, S^* = 1$		butatriene $n \geq 2$	A, B, C, ...	I, II, III, ...
—DC— dicarbenes $S = 0, S^* = 1, 2$		acetylene $n \geq 7$	—	i, ii, iii, ...
—AC— asymmetric carbenes $S = 1$		acetylene $n \geq 2$	a, b, c, ...	1, 2, 3, ...
—SO— stable oligomer $S = 0$		acetylene $n \geq 3$	$\beta, \gamma, \delta, \dots$	—

extraordinary solid state photoreaction. A classical partition of the individual reactions within the polymerization process into three different reaction types is possible. These are the chain initiation, the chain propagation, and finally the chain termination reactions.

2 The Intermediates of the Low Temperature Photoreaction

2.1 Optical Absorption Spectra

Optical absorption spectroscopy in the temperature regime between about 10 K and 300 K is usually performed using conventional optical absorption spectrometers (Cary, Phillips) and temperature variable helium gas flow cryostats. In order to initiate the polymerization reaction the diacetylene monomer crystals were excited into the $S_0 \rightarrow S_1$ absorption edge at about 310 nm using either a xenon high pressure arc or the 308 nm line of an excimer laser (ArF).

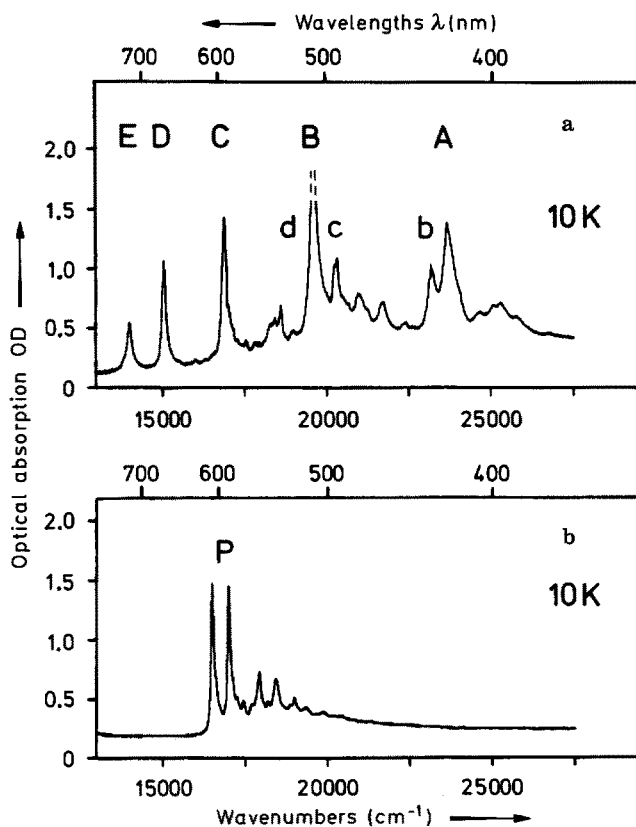


Fig. 4a and b. Optical absorption spectra of a diacetylene crystal (TS-6) at low temperatures. **a** Spectrum of the low temperature photoproducts obtained after UV-irradiation; **b** Spectrum of the polymer filaments obtained after thermal polymerization at 300 K at low degree of conversion (about 100 ppm)

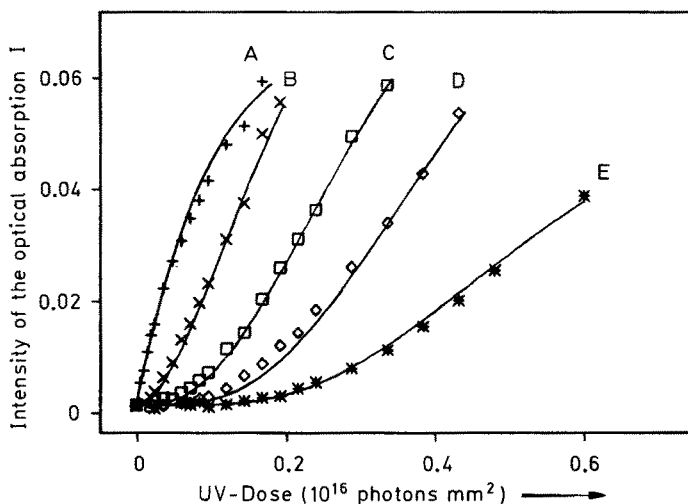


Fig. 5. Generation of the intermediates A to E obtained in the UV-photopolymerization reaction at 10 K. The intensity of the absorption lines is a function of the absorbed photons (proportional to the irradiation time). The calculated dependencies are fitted to the experimental points

The intense absorption lines of the photoproduct series A to E obtained by UV-irradiation at low temperature are shown in Fig. 4a⁴⁴). This spectrum represents a difference spectrum, where the original spectrum of the monomer crystal, certaining a small amount of polymer has been subtracted. Therefore only the effect of the UV-irradiation is shown in the Figure. In the same spectra lines b, c and d of a weaker series a to e are also present. For comparison the low temperature optical absorption of the polymer chains is shown in Fig. 4b. In a simple picture one would expect the positions of the optical absorption of the intermediates to be situated between the monomer and polymer absorption. However, lines D and E are below the polymer absorptions. In contrast to the absorptions at room temperature the polymer chain absorptions at low temperatures are split into doublets. This splitting is caused by a structural phase transition³⁵). The phase transition occurs at 170 K and results in a doubling of the unit cell in alignment with the chain direction. A corresponding doublet structure is also present in all absorptions of the reaction intermediates described in this paper, however, their intensity ratios are less than 1:10 and therefore in most cases a resolution of the weak lines is possible only after very intense UV-irradiation.

The generation sequence of the most intense photoproduct series is shown in Fig. 5 by the integral absorptions of the individual photoproducts as a function of the irradiation time⁴⁴). Only the photoproduct A is generated without any delay. In the sequence B, C, D, ... the induction period increases continuously. This corresponds to the expected polymerization reaction starting with the formation of the dimer A followed by subsequent addition reaction steps to the trimer B and tetramer C molecules etc. The curves are calculated using the kinetic expressions described below.

The series b, c, d, ... may be obtained in the same way by UV-irradiation (see Fig. 4a) but also in a transformation reaction by resonant optical bleaching of the series A,

B, C, ... at low temperatures. This transformation reaction is shown by example of the photoproducts A and b in Fig. 6. Upon 425 nm irradiation into the photoproduct A absorption of the A line is bleached and photoproduct b appears at the expense of A. The corresponding reactions are valid for B and c, C and d, etc.

Analogous to the photoreactivity of the A, B, C — series the b, c, d-series may be optically bleached. As a result a new series γ , δ , ϵ appears in the optical absorption spectra. This series is optically and thermally stable and therefore reacts neither upon UV-or resonant irradiation nor upon annealing of the crystal up to room temperature. This is in contrast to the intermediates A, B, C, ... and b, c, d, ... which finally form polymer chains.

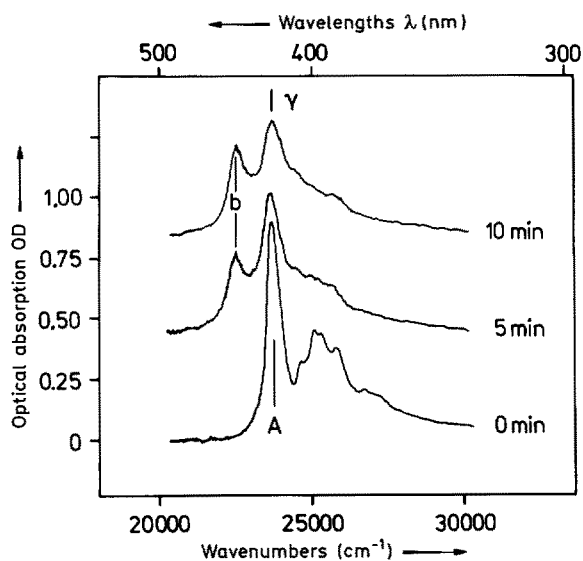


Fig. 6. Optical bleaching of the photoproduct A by resonant irradiation into the A absorption. The A absorption is transformed into the b and γ absorptions ($A \rightarrow b \rightarrow \gamma$)

The absorption lines of the low temperature photoreaction products in TS-6 monomer crystals are summarized in the diagram of Fig. 7. The correlation of the A, B, C, ... photoproduct series to diradical DR intermediates and of the b, c, d, ... photoproducts to asymmetric carbene AC intermediates is based on the ESR experiments discussed below. The correlation of the γ , δ , ϵ , ... series to stable oligomers SO is based on their thermal and optical stability. The correlation of dimer, trimer, tetramer, ... molecules follows from the chemical reaction sequences observed in the time resolved optical and ESR measurements as well as from the widths of the one-dimensional potential wells used in the simple "electron gas" theory^{68,69}, which already has proved successful in its application to dye molecules⁴⁵. Following Exarhos et al.⁴⁶ the explicit dependence is given by

$$E_n = \frac{h^2}{8ml^2} (4n + 1) + E_\infty \left(1 - \frac{1}{4n}\right)$$

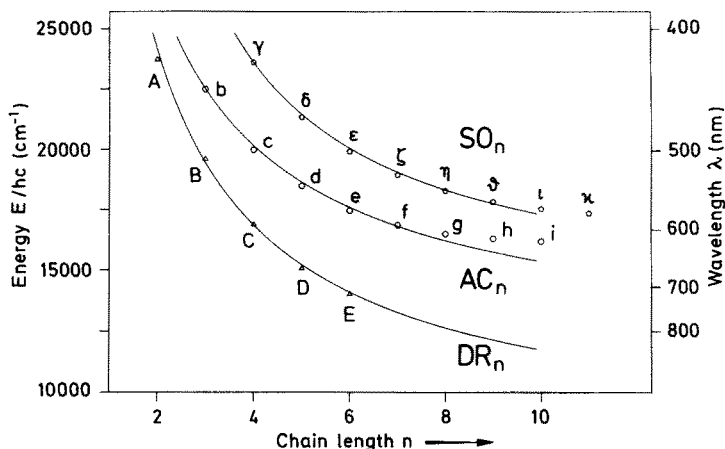


Fig. 7. Spectral position of the principal zero phonon absorption lines of the three photoproduct series as a function of the chain length n in monomer units. The calculated curves have been fitted to the experimental points. The data are given in Table 3

with

$$l = a_1 n + a_2 \quad (2)$$

h and m are Planck's constant and the electron mass, respectively. a_1 is given by the fixed lengths of the repetition unit and a_2 describes the boundary conditions at the ends of the oligomers. The excellent fit^{68, 69)} obtained by Eq. (2) supports the correlation of the different DR, AC and SO intermediates to distinct chain lengths n . There are neither excess nor missing intermediates. The deviations from the theory at long AC and SO chain length are not unexpected, since Eq. (2) is derived for equidistant carbon-carbon separations, best approximated only by the butatriene structure. The values used in the calculation are given in Table 3.

The convergence energies of the AC and SO series (see Table 3) are closest to the absorption energy of the polymer chain ($E_p \cong 17.000 \text{ cm}^{-1}$) and consequently are suspected of having related structures. However, the convergence of the DR series A, B, C, ... is strongly red shifted in comparison with the absorption of the polymer. The diradicals DR shown in Table 1 differ essentially from the other intermediates by their butatriene structure. Consequently, the modulation of the potential curves given by the atomic positions is changed. In accordance with the theory of Brédas

Table 3. Data used in the one-dimensional electron gas model calculation following Eq. (2)

	DR	AC	SO
a_1	5,39 Å	5,39 Å	5,39 Å
a_2	1,80 Å	2,10 Å	0
E_∞	6.600 cm^{-1}	9.700 cm^{-1}	11.200 cm^{-1}

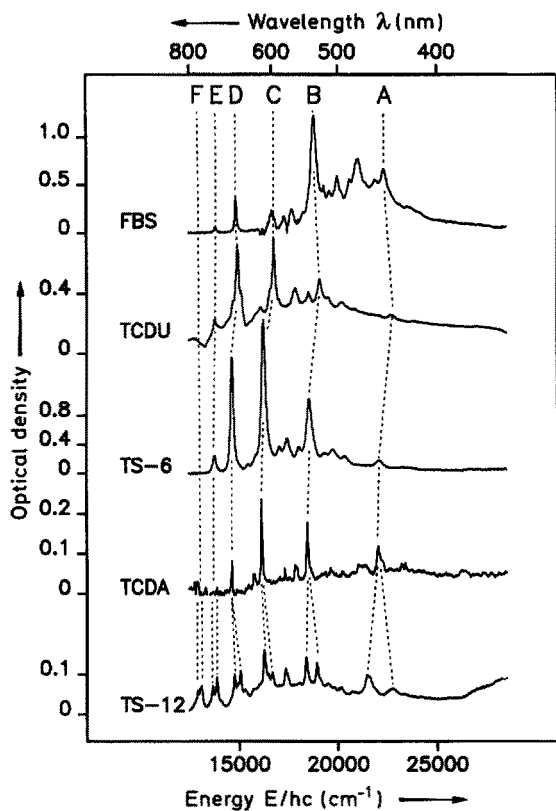


Fig. 8. Low temperature photo-product absorption in diacetylene crystals with different substituents

et al.⁷⁰⁾, distinctly lower values of E_{∞} for the butatriene structure of the DR series are expected as compared to the acetylene structure of the AC and SO series! The value of the absorption energy of the polymer chains in TS-6 crystals is in accordance with the proposed acetylene structure of the long polymer chains, as deduced from the original X-ray structure data^{34, 71)}. As will be shown later, the butatriene structure is favoured energetically as compared to the acetylene structure only at short chain lengths (photoproducts A to E) since no further longer butatrienic photoproducts F, G, H, ... could be detected in TS-6 crystals. As shown in Fig. 8 the DR- and AC-absorption series of the short oligomer units in TS-6 crystals are present also in the low temperature photoreactions in TS-12, TCDU, and TCDA crystals at almost the same spectral positions⁶⁹⁾, though the final positions of the polymer absorptions in these crystals are very different.

2.2 ESR Absorption Spectra

The ESR experiments are performed in an analogous manner to the optical experiments with the same low temperature and UV irradiation equipment using a conventional ESR spectrometer (9,3 GHz, Varian).

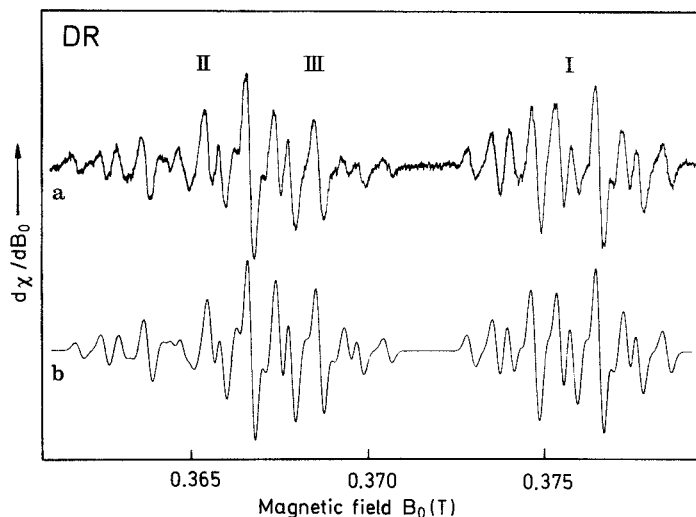


Fig. 9a and b. High field part of the triplet ESR spectrum of the diradical series (77 K). **a** experimental spectra; **b** simulated spectra. The correct hyperfine pattern is obtained by the interaction with two CH_2 -groups

The high-field ESR spectrum of the most intense ESR signals of the diradical DR series I, II, III obtained after UV-photoinitiation of the low temperature polymerization reaction is shown in Fig. 9a. This spectrum is part of a typical triplet ESR spectrum with spin quantum number $S = 1$ which consists of two ESR lines with $\Delta m = \pm 1$. The splitting of the ESR line pairs (the low-field lines are not shown in the Figures, see e.g. Ref. ⁵⁶) is the fine-structure splitting due to the magnetic dipolar interaction of the two electron spins, which are electrostatically coupled to form either triplet states or singlet states. Due to the doubling of the unit cell in the low temperature phase of the TS-6 crystals the ESR spectra show a further line splitting (analogous to the splitting of the polymer absorption in Fig. 4b) which is not relevant for our purposes.

The temperature dependence of the individual ESR lines is shown in Fig. 10. The reversible disappearance of the lines at low temperatures clearly demonstrates a thermal activation of the triplet species. Optimum signal intensities are obtained at about 77 K (see Fig. 9a). The temperature dependence of the individual lines is best described by the energy level system shown in Fig. 10 with a singlet $S = 0$ ground state and an activated triplet state. The corresponding intensity dependencies are given by $I(T) \propto x/(3 + e^x)$ with $x = E_T/kT$ (k is Boltzmann's constant) shown by the curves in Fig. 10. The activation energies E_T of the triplet states are obtained from the optimal fit of the curves. They are different for the individual triplet states and lie between 7 and 14 meV ⁵⁶. The temperature dependence of the ESR signal intensities is reversible only below 80 K. At higher temperatures the ESR signals disappear irreversibly due to the thermal reactions which finally lead to polymer filaments.

The hyperfine interactions arise from the magnetic dipolar coupling of the triplet electrons with the protons (nuclear spin $I = 1/2$) within the CH_2 -groups of the sub-

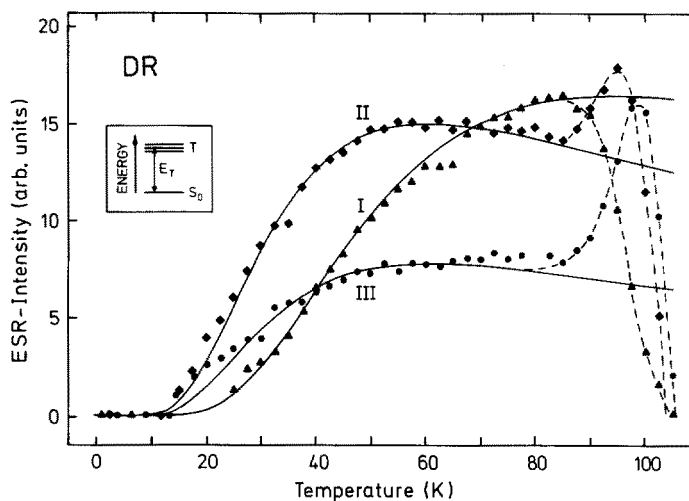
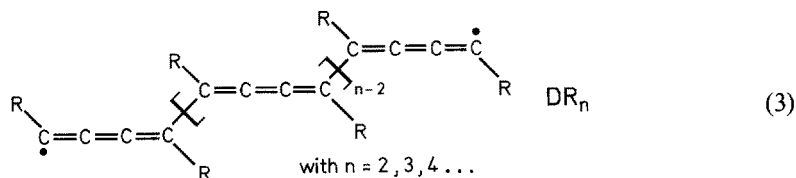


Fig. 10. Temperature dependence of the diradical spectra. The calculated temperature dependencies using the inserted energy level diagram has been fitted to the experimental points

stituents $R = CH_2R'$ which link the substituents to the diacetylene unit. The hyperfine splitting of the ESR lines has been analyzed by computer simulation. The calculated spectra of Fig. 9b are based on a hyperfine interaction with only two identical CH_2 -groups located at the two ends of the oligomer units.

Owing to the low values of their fine structure parameters and to their characteristic hyperfine pattern the thermally activated triplet states I, II, III, ... are identified as diradical DR oligomers with the following symmetric butatriene structure:



This structure is in accordance with the optical absorption spectra, where a sequence of butatriene chain structures with increasing n was postulated as responsible for the red shift of the absorption lines A to E (see Fig. 7). The longest diradical molecule (which has been detected in the optical system) therefore is the hexamer E with $n = 6$. For each value of n further mesomeric butatriene and acetylene structures are present up to maximally 10% of the real structure of the diradicals.

By analogy to the optical absorptions A to E (see Fig. 5) the kinetical generation sequence of the diradical oligomers I to III obtained upon UV-irradiation of the monomer crystals is shown in Fig. 11⁶²). Only the ESR line I is formed without any delay. The curves are calculated using the kinetic model described below. In this model the ESR line I corresponds to the DR dimer molecule, II to the DR trimer molecule, etc.

Parallel to the generation of the DR oligomers carbenoid AC oligomers (see Table 2) are formed upon UV-irradiation of the monomer crystals at low temperatures. The high field part of the AC triplet ESR spectra with the lines 1, 2, 3, and 4 is shown in Fig. 12. The unspecified lines are not relevant for our purposes; they are attributed to the doubling of the unit cell in the low temperature phase of the TS-6 crystals³⁵.

In contrast to the DR triplets, the AC triplets are in their electronic ground state. This follows from the $1/T$ Curie law temperature dependence of the ESR intensities. The fine structure splitting and the pattern of the hyperfine structure of the DR and

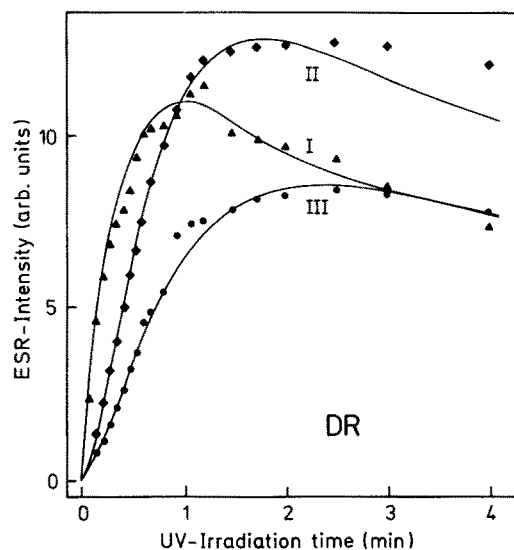


Fig. 11. Diradical formation upon UV-irradiation. The calculated dependencies have been fitted to the experimental points

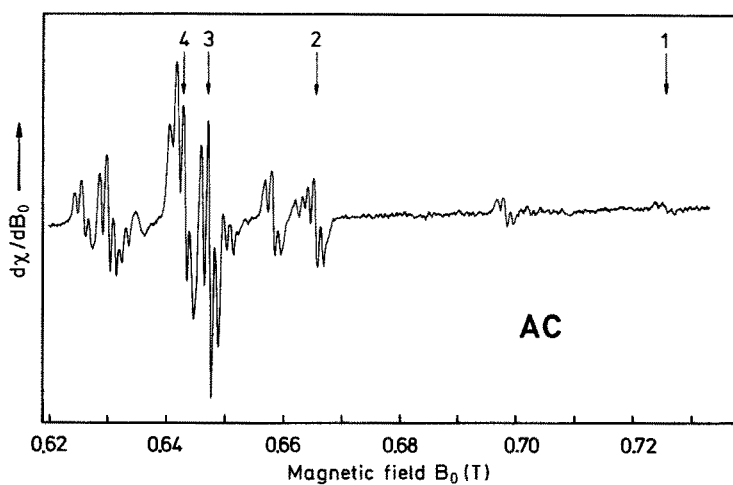


Fig. 12. High field part of the triplet ESR spectrum of the asymmetric carbenes. Only the high field partners of the pair lines have been assigned by the numbers

any delay. The curves are calculated using the kinetic model described below. In this model the ESR line 1 corresponds to the AC dimer molecule, 2 to the AC trimer molecule etc.

Besides the direct generation of the monomer crystals by UV-irradiation AC molecules may also be produced indirectly by optical bleaching of the DR molecules. This has been demonstrated by example of the optical absorption $A \rightarrow b$ in Fig. 6. The corresponding transformation of the ESR lines $1 \rightarrow 2$ during optical bleaching of $A \rightarrow b$ is shown in Fig. 14. The dimer DR molecule I is *not* transformed to the dimer AC molecule 1 but to the trimer AC molecule 2. Consequently, one monomer molecule is added in each resonant phototransformation reaction of DR molecules to AC molecules.

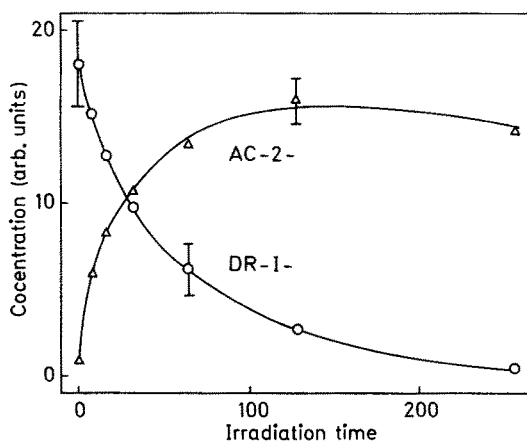


Fig. 14. Transformation of the diradical ESR line 1 to the asymmetric carbene ESR line 2 upon resonant irradiation into the photoproduct A absorption. The concentration of the triplet species has been deduced from the evaluation of the ESR spectra

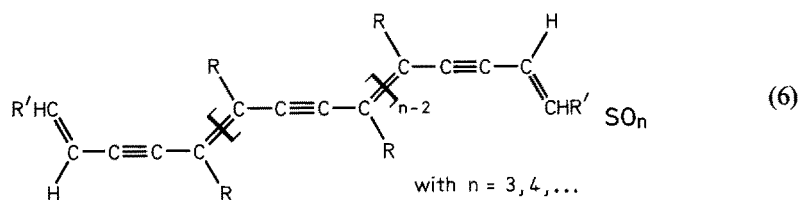
2.3 Correlation of the Photoproducts

The resonant phototransformation reaction allows a clear correlation of the optical and ESR spectra: The series A, B, C, ... and I, II, III correspond to the same diradical DR photoproducts with butatriene chain structure. The series a, b, c, ... and 1, 2, 3 correspond to the same asymmetric carbene AC photoproducts with acetylene chain structure. The identification of the dimer molecules $DR_2 = A = I$ and $AC_2 = a = 1$ is based on their spectral positions, on the generation, addition and transformation properties, and on their quadratic photoinitiation process discussed below. The identification of the trimer ($DR_3 = B = II$ and $AC_3 = b = 2$) and tetramer molecules, etc. follows the same lines. The longest detectable DR oligomer is the photoproduct E which is the hexamer molecule with $n = 6$. In TS-12 crystals²⁷⁾ the longest DR oligomer is the heptamer with $n = 7$. Longer DR units are unstable. As will be shown below they are transformed to dicarbene DC molecules. The longest detectable AC oligomer molecule is the photoproduct i with $n = 10$. Longer AC oligomers probably occur but are not resolvable, due to the convergence of the optical absorption spectra.

The asymmetric AC species are composed of a reactive carbenic chain head and an unreactive chain tail with fully saturated bonds. They are formed by optical transformation of the diradical molecules DR_n : In a first chain termination reaction one reactive chain end is destroyed and an unreactive chain end is formed by addition of a monomer molecule following $DR_n \rightarrow AC_{n+1}$. In a second chain termination reaction the remaining reactive chain end of an AC oligomer may be destroyed in a further photoaddition reaction. In this way the AC oligomers are transformed to stable oligomers SO (γ , δ , ϵ , ...) with two unreactive chain ends. This transformation reaction has been observed in the optical spectra. As expected no corresponding ESR spectra could be detected since radical electrons were absent.

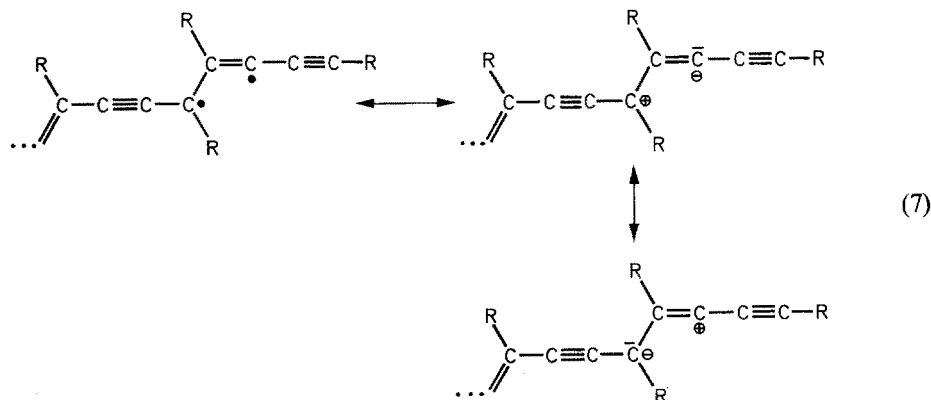
The correlation of the stable oligomers observed in the optical spectra (see Fig. 7) to trimer ($\beta = SO_3$), tetramer ($\gamma = SO_4$), pentamer ($\delta = SO_5$) molecules etc. is based on the $AC_n \rightarrow SO_{n+1}$ transformation process. From the convergence of the optical absorption lines (see Fig. 7) an acetylene structure of the SO backbone similar to that of the AC oligomers is very likely.

The structure of the SO molecules therefore is best represented by



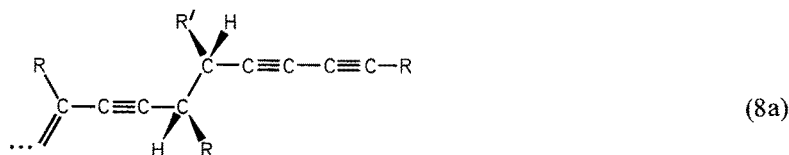
So far the structure of the unreactive SO chain ends has not been clearly proved.

Three essentially different stable chain end configurations have been suggested. The following mesomeric planar pseudocyclopropan structures (7) with bond length up to 1,6 Å have been suggested by Wegner⁵⁸⁾.

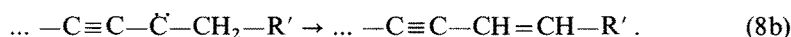


The following nonplanar methylene-group binding, which is formed by an intermolecular insertion reaction of the reactive radical chain end into a CH-bond of

the rest group $R = \text{CH}_2\text{R}'$ of an adjacent monomer molecule has been suggested by Bubeck⁷⁷⁾.



The unreactive chain end structures of the AC_n and SO_n molecules shown in Eqs. (5) and (6) are obtained by an intramolecular insertion reaction given by



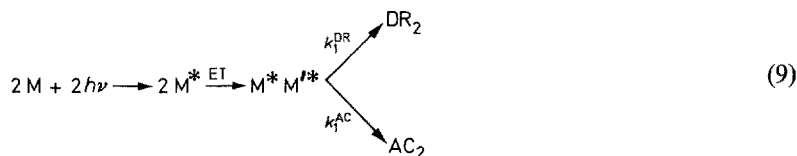
All structures (7) and (8) are hypothetical, because up to now no final proof of the structures — for example by analysis of the vibronic structures or by chemical shift measurements — has been given. The reactions leading to the discussed structures (7) and (8) are typical carbene reactions^{78, 79)}.

2.4 The Individual Steps of the Low Temperature Photopolymerization Reactions

Following the experimental absorption data a classical partition of the low temperature photopolymerization reaction is possible. The individual reaction steps are given by the photoinitiation reaction (formation of reactive dimers), the photoinduced chain propagation (addition of monomer molecules to the reactive oligomers), and the photoinduced chain termination reaction (formation of unreactive chain ends). As shown in the optical and ESR experiments the dimer DR_2 and AC_2 formation is quadratically dependent on the UV-light intensity^{62, 63)}, whereas both the chain propagation and the chain termination reactions are linearly dependent on the intensity. Therefore, the dimer photoinitiation is a bimolecular reaction in contrast to the monomolecular photoaddition reactions, leading to chain propagation or chain termination.

In the bimolecular chain initiation reaction two monomer molecules must first be photoexcited according to $2\text{M} + 2h\nu \rightarrow 2\text{M}^*$. Then via energy transfer ET processes the excitation energy (which may be of excitonic, vibronic, librionic, or phononic character) must be transferred to the immediate neighbourhood of the reaction center. As will be shown later (see Section 4) the reactive centre has a radical structure (which is obtained by electronic excitation of the monomer molecules M^*) whereas the second excitation encountering the adjacent molecules M' of the reaction centre need not necessarily be of radical nature. The energy transfer is described by $\text{M}^*\text{M}' + \text{M}^* \rightarrow \text{M}^*\text{M}'^* + \text{M}$. From the ESR experiments the reaction yields of the DR_2 and AC_2 dimer molecules are given by approximately 10:1. The low concentration of the AC_2 centres (denoted by 1) and the energetic position of the corresponding optical absorptions close to that of the monomer explains their apparent absence from the optical spectra.

The photoinitiation reactions are described by the following reaction Equation:



The photoinitiation reactions is possible only upon excitation of the monomer molecules M^* of the monomer crystal. No further dimer formation is possible when the crystal is irradiated below the monomer absorption band located at 310 nm.

Parallel to the photoinitiation processes (with $h\nu$) photoaddition processes are observed, as shown for example in the Figs. 4, 5, 11 to 13. After dimer initiation, trimer formation from the dimer is possible etc. The chain propagation within the DR or AC series is performed by photoaddition of monomer molecules M' adjacent to the reaction centres, given by the dimer (DR_2 or AC_2), trimer (DR_3 or AC_3), ... molecules. The molecules M' are lowered in energy by the perturbation introduced by the reaction centres. They form a trap for the optical excitation energy. They may be excited directly ($M' + h\nu' \rightarrow M'^*$) or indirectly via nonperturbed monomer molecules ($M + h\nu \rightarrow M^*$) and subsequent energy transfer ($M^* + M' \xrightarrow{ET} M + M'^*$). The chain propagation reaction therefore is in competition with the chain initiation reaction.

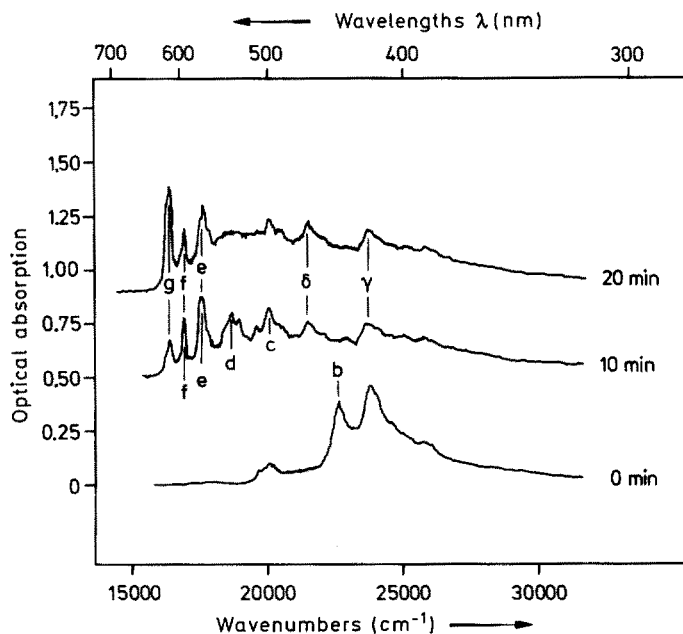
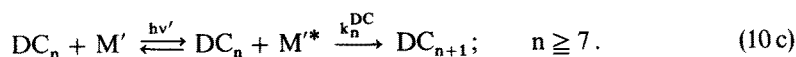
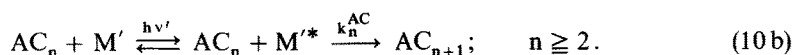
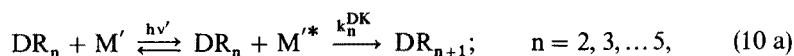


Fig. 15. Optical addition polymerization of the AC series b to g upon 364 nm irradiation of the TS-6 crystal. The initial spectrum at 0 min corresponds to the final spectrum of Fig. 6. In addition transformation reactions to the γ , δ -series are observed

Direct excitation of the molecules M' is performed with UV-light energies below the monomer absorption edge $h\nu' < h\nu$ (with wavelength $320 \text{ nm} < \lambda < 370 \text{ nm}$). The photoaddition polymerization reaction obtained in this way at 10 K is shown for the optical absorptions of the AC-centres (b, c, d, ...) in Fig. 15. After preparation of the b photoproduct (see the procedure of Fig. 6) the sequence of the AC centres $b \rightarrow c \rightarrow d \rightarrow e \rightarrow f \rightarrow g$ is obtained upon 364 nm-irradiation. Simultaneously chain termination reactions leading to the stable oligomers δ and ϵ are observed. The same reactions are also observed with the diradicals in the ESR and optical spectra. After preparation of the dimer diradical and subsequent 364 nm-irradiation, very effective addition polymerization reactions are observed parallel with chain termination reactions leading to AC-molecules. The same effects are valid for the dicarbene DC species described below (Section 3.2).

The photoinduced chain propagation by addition of adjacent monomer molecules M' to the DR, AC and DC reaction centres is described by the following reaction Equations:

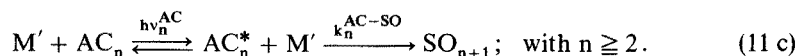
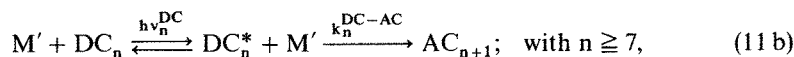
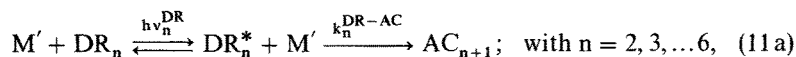


No back reactions ($n \rightarrow n - 1$) have been observed in the experiments.

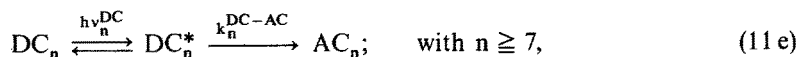
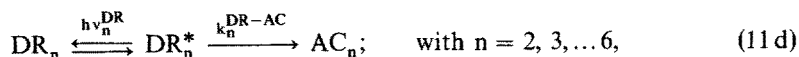
Parallel to the photoinitiation (with $h\nu$) and to the photoaddition reactions (with $h\nu$ and $h\nu'$), chain termination reactions are observed as shown, for example, in Figs. 4, 6 and 15. In the chain termination reactions the radical character of the chain ends is destroyed in a photoaddition reaction as shown by Eqs. (5) to (8).

The chain termination reactions are performed most effectively by resonant optical excitation of the DR and AC intermediates (optical bleaching) as shown in Figs. 6 and 14. The DR and AC reaction centres may be indirectly excited via energy transfer from the monomer matrix. The chain termination reactions are, therefore, in competition with the photoinitiation and photoinduced chain propagation reactions.

The chain termination reactions involving an intermolecular insertion reaction are described by the following reaction Equations.



In the case of an intramolecular insertion reaction (8b) no addition of a monomer molecule is expected upon chain termination



The destruction of the first reactive chain end leads to AC oligomers. The destruction of the second reactive chain end leads to SO oligomers. No back reactions ($n \rightarrow n - 1$) have been observed in the experiments.

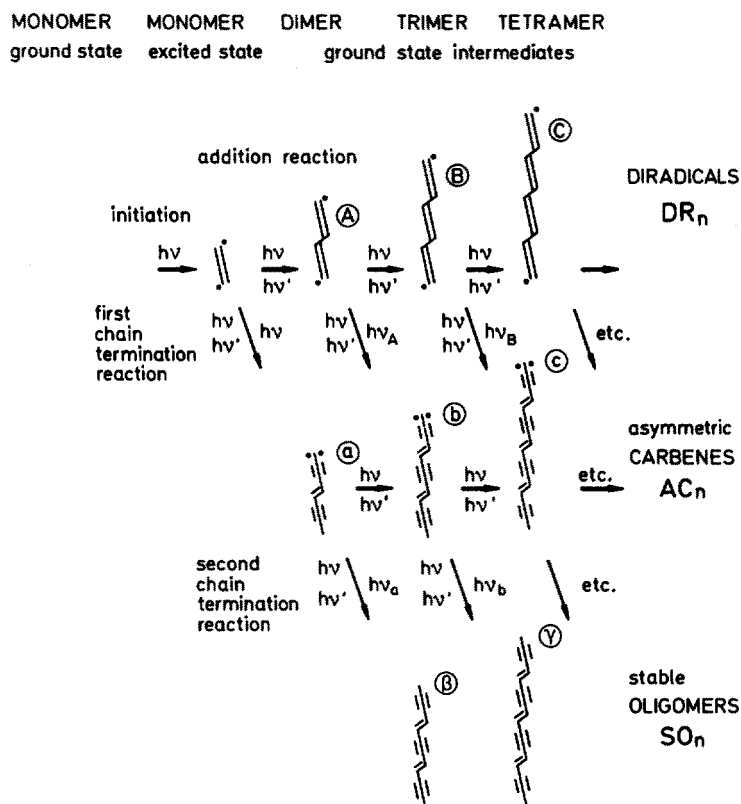


Fig. 16. Photoreactions at low temperatures. The notation corresponds to the optical absorption lines of the reaction intermediates. An intermolecular chain termination reaction is assumed. The dimer initiation reaction requires two photons ($h\nu$). The photoaddition reaction is a one photon process ($h\nu$ or $h\nu'$). The chain termination reactions are most effectively performed by resonant irradiation into the absorption of the DR or AC intermediates

2.5 Reaction Scheme of the Low Temperature Photoreactions

A reaction scheme showing the individual steps of the low temperature photopolymerization reaction of the DR and AC reaction intermediates and of the SO, which are the final reaction products, are taken from the optical absorption spectra. All molecules shown in Fig. 16 have been observed in either the optical spectra or ESR-spectra or in both with the exception of only the short lived monomer species. The reactive chain ends are best represented by the diradical and carbene structures, shown in the Figure.

The photoinitiation is a two step reaction: Two photons of energy $h\nu$ are involved in the DR or AC dimer formation. Subsequent photoaddition polymerization reaction in the DR or AC sequence are given by the horizontal arrows. They are possible with photons of energy $h\nu$ or $h\nu'$. Chain termination reactions are given by the diagonal arrows. In these reactions the reactive chain ends are transformed to nonreactive chain ends by resonant absorption of light quanta with energy $h\nu_n$ or via energy transfer with $h\nu$ or $h\nu'$. In the reaction scheme it is assumed that monomer molecules are added in the chain termination reaction according to (11a-c).

3 Thermal Reactions of the Low Temperature Photoproducts

3.1 Optical Absorption Spectra

The DR and AC intermediates of the photopolymerization reaction are stable only at low temperatures. At temperatures above about 100 K they react to form long macromolecules by subsequent addition of monomer molecules. The 10 K optical absorption spectra of Fig. 17 show the result of the thermal reaction as a function of the time at 100 K⁶⁹⁾. The initial spectrum showing only the dimer A absorption has been prepared at 10 K by only one UV-excimer laser pulse at 308 nm. Only pure thermal addition polymerization reactions are observed within the DR-series A, B, C, ... No chain termination reactions are detectable in the optical spectra. The final product P' is situated in the vicinity of the final polymer absorption.

Analogous to the DR series the optical absorption spectra of the AC series also shows pure thermal addition polymerization reactions within the AC series b, c, d, ... The final product P'' (different from P') is also situated in the vicinity of the polymer absorption. The AC intermediates are slightly more reactive than the respective DR intermediates of equal length. The thermal reactions of the AC intermediates generally start at lower temperatures than the DR intermediates. Within a series the short oligomer molecules are more reactive than the longer ones, presumably due to the increasing displacement of the chain ends originating from the different lattice parameters of the monomer and the polymer crystals.

The absorptions of the SO-oligomers γ , δ , ϵ are both, thermally and optically stable. Therefore upon thermal annealing up to room temperature and upon UV and resonant irradiation no reactions could be observed⁶⁹⁾. These oligomer molecules can be prepared optically only at low temperatures and are the only photoproducts which remain stable at 300 K. After preparation they may be dissolved from the

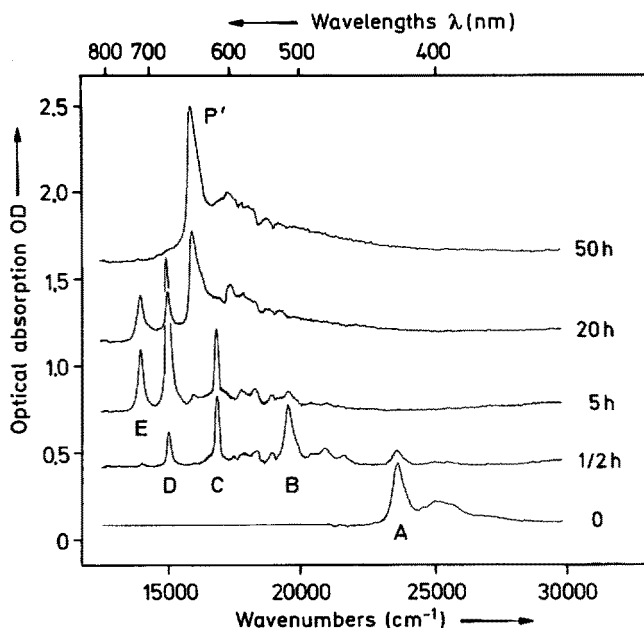


Fig. 17. Thermal addition reactions of the diradical series A to E at 100 K as a function of the annealing time. Optical absorption spectra

partially polymerized monomer crystal at room temperature and may be investigated in future experiments in solution with physical and chemical methods. Short trimer, tetramer, ... SO molecules cannot be prepared at high temperatures, due to the very efficient thermal addition polymerization following the photoinitiation reaction. The SO chain lengths distribution, obtained at about 300 K, is supposed to have its maximum at high chain length ($n > 50$), owing to the low chain termination yield in the thermal reactions.

3.2 ESR-Spectra

In analogy to the procedure of the optical spectra the thermal addition polymerization reaction is also observed in the ESR-spectra of the triplet DR and AC reaction intermediates⁶³. In the temperature dependencies of the AC and DR centres of Fig. 18 the temperature has been increased continuously. The initial slight increase of the DR ESR signals in Fig. 18a characterizes the thermally activated DR triplet states. The chemical reactions start at about 95 K. The initial slight decrease of the AC ESR signals in Fig. 18b is given by the $1/T$ Curie law of the AC triplet ground states. The chemical reactions start at about 90 K.

The thermal reactions of the DR-intermediates, however, exhibit an extraordinary effect. Hand in hand with the disappearance of the DR series a new series appears, which shows a four line ESR fine structure arising from $S = 2$ quintet dicarbene DC states⁶³⁻⁶⁶. The thermal transformation of the DR intermediates into the DC inter-

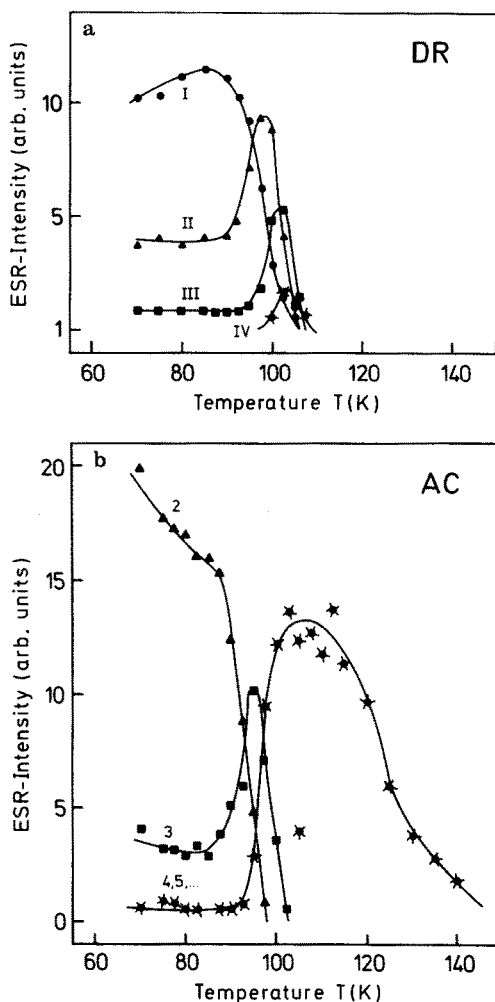


Fig. 18a and b. Thermal addition reactions of the diradicals (a) and of the asymmetric carbenes (b) as a function of the temperature. ESR intensities

mediates is shown in Fig. 19 as a function of the annealing time at 90 K. At 100 K the individual DC oligomers react in turn by thermal addition reaction steps to longer DR oligomers. The longest DC oligomers cannot be distinguished from the AC triplet states due to the convergence of the DC-ESR spectral lines which occurs at the same position of the long AC triplet states. In contrast to the photoinduced addition reactions no chain termination reactions could be clearly proved.

Analogous to the triplet DR-spectra the quintet DC-spectra are thermally activated. The temperature dependence of the individual quintet ESR intensities $I(T)$ could be fitted with a singlet $S = 0$ ground state and an activated quintet state. The corresponding dependencies are given by $I(T) \propto x/(5 + e^{-x})$ with $x = E_Q/kT$ ⁶³⁻⁶⁶. The activation energies E_Q of the quintet states (obtained from the optimal fit of the curves) are different for the individual quintet states and are extremely low in energy. As shown in Fig. 20 ⁶⁷ they lie between about 30 μeV and about 10 meV. The quintet ESR intensities are reversible only below 80 K.

The fine structure and the hyperfine structure of the DC intermediates has been investigated in detail by ESR⁶³⁻⁶⁶⁾ and ENDOR spectroscopy⁶⁷⁾. Fig. 21 shows the angular dependence of the ESR resonance fields with B_0 approximately perpendicular to the oligomer chain direction. The curves represent the calculated

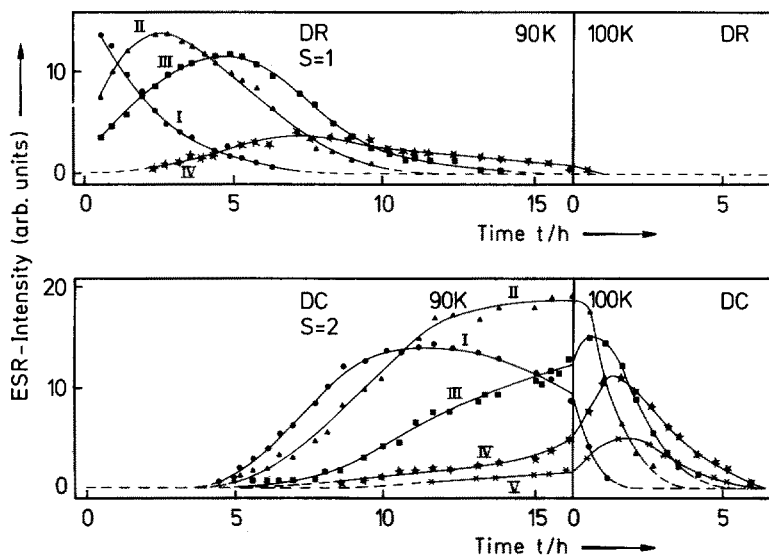


Fig. 19. Thermal addition and transformation reaction of the diradicals DR to the dicarbenes DC. The formation and the decay of the ESR intensities is given as a function of the time of thermal annealing at 90 K resp. 100 K.

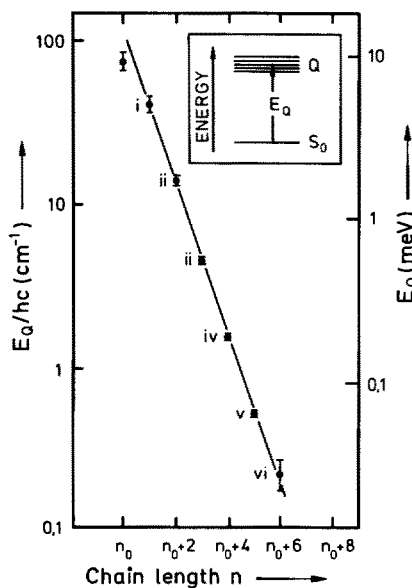


Fig. 20. Experimental values^{67, 83)} of the singlet-quintet activation energies as a function of the lengths of the dicarbene molecules. The first DC molecule presumably is the heptamer with $n_0 = 7$

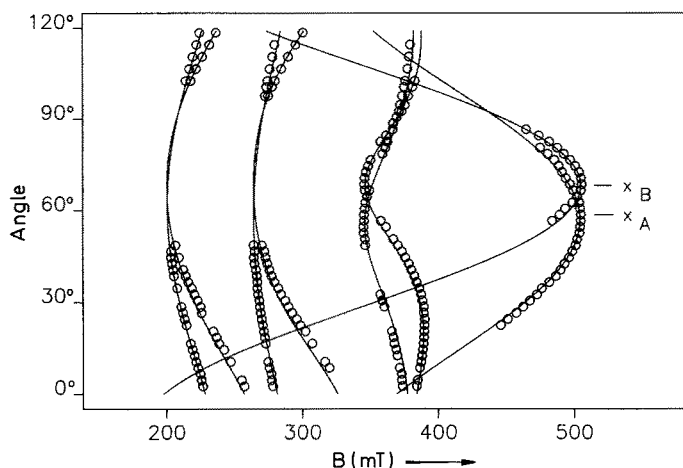
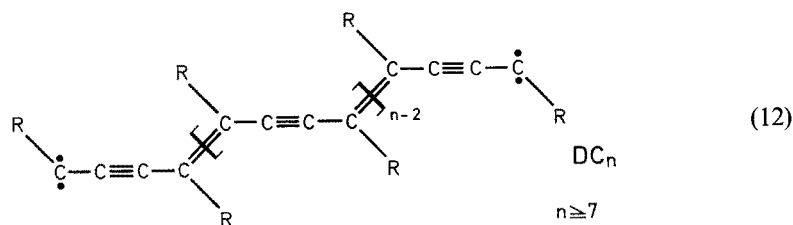


Fig. 21. Angular dependence of the four $\Delta m = 1$ ESR transitions of a DC-quintet state (I)

angular dependencies of the four $\Delta m = 1$ transitions of a $S = 2$ dicarbene quintet state. The hyperfine structure analysis⁶⁷⁾ of the ESR lines leads to the following symmetric dicarbene structures:

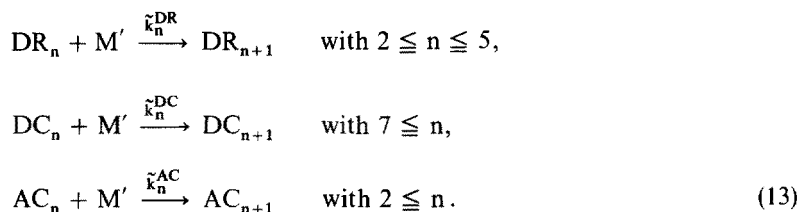


The individual chain ends of the DC intermediates exhibit the same mesomeric structures (4) of the corresponding asymmetric carbenes AC and a carbon backbone with acetylene structure. It has been shown in a quantitative theory of the DC quintet states^{66, 80, 81)}, that the fine structure parameters D_Q of all DC intermediates are given by the fine structure parameters D_T of two AC-oligomers with $n \approx 4$. Therefore in accordance with the disappearance of the DR intermediates at $n > 6$ it is concluded that the shortest DC intermediates are either heptamer or octamer molecules. The different activation energies E_Q of the quintet states are due to the electron exchange interaction between the electrons of the carbene pair⁸²⁾. The larger the distance between the carbene pair the lower the exchange interaction and the lower the energy separation between the singlet ground state and the quintet excited state (see Fig. 20). As a consequence the singlet and quintet states become mixed⁸⁰⁾, resulting in a dramatic but continuous change of the fine structure splitting. The different DC-molecules with lengths up to 5 nm may be easily resolved in the ESR spectra due to the low value of E_Q which acts as an additional fine structure parameter. Up to seven differently long DC intermediates have been detected by W. Neumann and R. Huber^{66, 67)}. The lengths of the DC oligomers therefore range between $7 \leq n \leq 14$

diacetylene units and are impossible to resolve in the optical spectra, due to the convergence of the spectra for long diacetylene units (see Fig. 7). In addition, the corresponding optical absorptions are expected to lie at positions close to the AC-intermediates, due to the related acetylene chain backbone.

3.3 The Thermal Reaction Steps

The *thermal addition reactions* following the photochemical dimer initiation reaction are described by the following reaction equations for the relevant, thermally reactive intermediates:



The rate constants of the thermal reactions are denoted by \tilde{k} . Back reactions have not been observed. No chain termination reactions could be identified in the thermal addition reactions in contrast to the optical addition reactions. The average length of the SO oligomers obtained in the thermal chain termination reactions is estimated to be of the order of $n \approx 150$ units.

The temperature dependent thermal reaction constants \tilde{k}_n describe both the decay of the n -mer molecules, and by the addition step to DR_{n+1} , the generation of the $n+1$ -mer molecules. Consequently in Figs. 18 and 19 only the dimer molecules (I) decay monoexponentially. The trimer and tetramer molecules etc. (I, II, etc.) are first produced from their precursors before decaying. Their time dependencies are described by two or more exponential functions.

The activation energies E_a of the thermal addition reactions are determined by the temperature dependent reaction constants, defined by

$$\tilde{k}(T) = \tilde{k}(\infty) \exp(-E_a/kT). \quad (14)$$

$\tilde{k}(\infty)$ are the temperature independent frequency factors. Because the values of \tilde{k} are expected to be different for all DR, AC and DC intermediates of different lengths, a series of activation energies E_a is expected, with the highest activation energy determining the overall activation energy of the polymerization process.

The temperature dependent generation and decay constants (14) of the reaction intermediates are obtained by an analysis of the time dependencies of the intensities of the optical absorption and ESR lines at the respective fixed temperatures. First investigations of this matter have been performed by Niederwald⁵¹⁾ and Neumann⁸³⁾ with the dimer diradical A ($180 \text{ K} < T < 300 \text{ K}$) and I ($80 \text{ K} < T < 100 \text{ K}$). By example of the DC ESR signals it may be seen from Fig. 19 that a small increase of the temperature from 90 K to 100 K results in an increase of the reaction rates by about one order of magnitude.

The temperature dependencies of the reaction constants \bar{k} determined from the polymerization rates are shown in Fig. 22. The dependencies (4) and (5) characterize the temperature dependencies of the reaction constants \bar{k}_2^{DR} of the dimer diradicals in the thermal addition reaction to the trimer. The DR_2 molecules (A and I) have been photoinitiated by one UV pulse of an excimer laser. The evaluation of the results of Niederwald^{51,52)} and Neumann⁸³⁾ yields an activation energy of $E_a \approx 200$ to 300 meV for the different short ($n \leq 4$) DR oligomers.

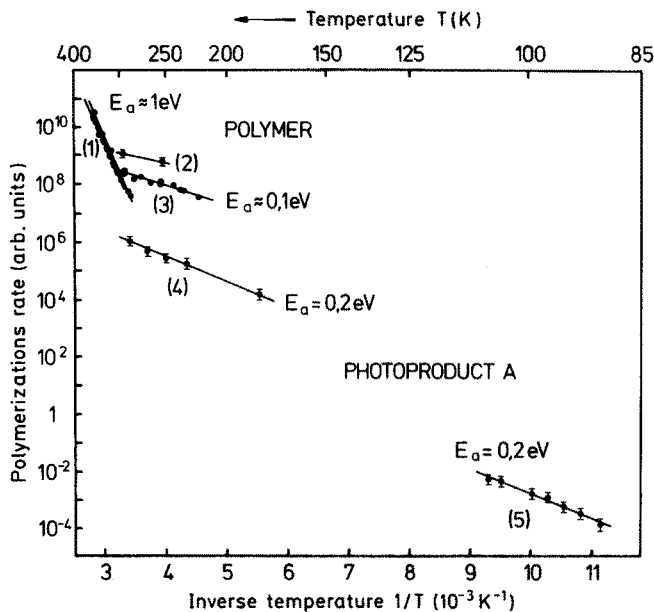


Fig. 22. Summary of recent results concerning the determination of activation energies. (1) Thermal polymerization⁶¹⁾; (2) γ -polymerization⁶¹⁾; (3) to (5) UV-polymerization^{51,52,61,83)}

Figure 22 includes the temperature dependent polymerization rates (1), (2) and (3). The thermal polymerization kinetics (1), the γ — (2), and the UV photopolymerization kinetics (3) have been investigated by the method of diffuse reflection spectroscopy⁶¹⁾ and other methods⁸⁴⁾. The activation energy of the thermal reactions (2) and (3) following the photoinduced dimerization processes, (150 ± 30) meV, is appreciable lower than those of the dimer DR intermediates. However, the processes which dominate the polymerization reaction are determined not by the short diradicals with $n \leq 6$ but by the long chains with $n \geq 7$, which all have a carbenoid DC or AC structure. The discrepancy of the activation energies therefore may be due to the different reactivities of the diradical and carbenoid chain ends. The activation energies of the thermal addition reactions of the AC and DC intermediates at low temperatures have not been determined and therefore a direct comparison with those of the diradicals is not possible.

In contrast to the thermal addition reactions (following the photodimerization) the high activation energy of the *purely thermal* polymerization reaction (without

photoinduced dimerization) is not determined by the thermal addition steps, having low activation energies as seen above, but solely by the thermal dimer or trimer initiation process of the polymerization reaction, which will be discussed below.

4 Kinetics

4.1 Rate Equations

For a quantitative calculation of the time dependencies of the concentrations of the intermediates $[DR_n]$, $[DC_n]$, $[AC_n]$, and of the stable oligomers $[SO_n]$ observed during the photochemical and thermal reactions in the course of the solid state polymerization reaction we still have to solve the corresponding rate equations. These are differential equations of first order and follow from the reaction Eqs. (9) to (13).

The *photoinitiation* reaction (ϕ) is defined by the reaction Eq. (9). The dimer generation rates G_2 of the diradical and asymmetric carbene dimer molecules are therefore given by the bimolecular rate equations

$$G_2^{\text{DR}}(\phi) = k_1^{\text{DR}}[M'^*][M^*] \quad \text{and} \quad G_2^{\text{AC}}(\phi) = k_1^{\text{AC}}[M'^*][M^*]$$

with

$$G_2^{\text{DR}} = d[DR_2]/dt \quad \text{and} \quad G_2^{\text{AC}} = d[AC_2]/dt . \quad (15)$$

The concentration $[M^*]$ of the excited monomer molecules is proportional to the absorbed light intensity. Owing to the increasing oligomer concentrations, $[M^*]$ decreases at constant light intensity, due to energy trapping in the oligomer states following $M^* + M_n \rightarrow M + M_n^*$ (M_n = oligomer molecules).

Chain propagation by addition of molecules starts with the reactive dimer molecules DR_2 and AC_2 . Below about 80 K addition of molecules is possible photochemically only upon excitation of the perturbed monomer molecules adjacent to the reactive chain ends of the intermediates. The photoaddition reactions are defined by the reaction Eq. (10a-c). The generation and decay rates $G = d[RO]/dt$ and $D = -d[RO]/dt$ of the individual reactive oligomer molecules $RO = DR, AC, DC$ of lengths n are given by:

$$\begin{aligned} G_n^{\text{RO}}(\text{pha}) &= k_{n-1}^{\text{RO}}[RO_{n-1}][M'^*], \\ D_n^{\text{RO}}(\text{pha}) &= k_{n-1}^{\text{RO}}[RO_{n-1}][M'^*], \end{aligned} \quad (16)$$

The concentration of the excited perturbed monomer molecules at the reactive chain ends $[M'^*]$ is directly proportional to the absorbed light intensity. In the case of indirect excitation via energy transfer ($M^* + M' \rightarrow M + M'^*$) it is proportional to the concentration of the excited unperturbed monomer molecules $[M^*]$.

At temperature above 80 K thermal reactions are observed. The chain propagation by *thermal addition (tha)* of monomers to the reactive intermediates is described

by the reaction Eq. (13) with the following reaction rates:

$$\begin{aligned} G_n^{\text{RO}}(\text{tha}) &= \bar{k}_{n-1}^{\text{RO}}[\text{RO}_{n-1}], \\ D_n^{\text{RO}}(\text{tha}) &= \bar{k}_n^{\text{RO}}[\text{RO}_n]. \end{aligned} \quad (17)$$

Photochemical chain termination reactions (pht) are produced by resonant irradiation into the corresponding optical absorption bands of the reactive intermediates. Corresponding to the reaction Eq. (11) the following rates are obtained:

$$\begin{aligned} G_n^{\text{AC}}(\text{phu}) &= k_{n-1}^{\text{DR-AC}}[\text{DR}_{n-1}^*] \quad \text{or} \quad G_n^{\text{AC}}(\text{phu}) = k_n^{\text{DR-AC}}[\text{DR}_n^*], \\ D_n^{\text{DR}}(\text{phu}) &= k_n^{\text{DR-AC}}[\text{DR}_n^*], \quad \text{etc.} \end{aligned} \quad (18)$$

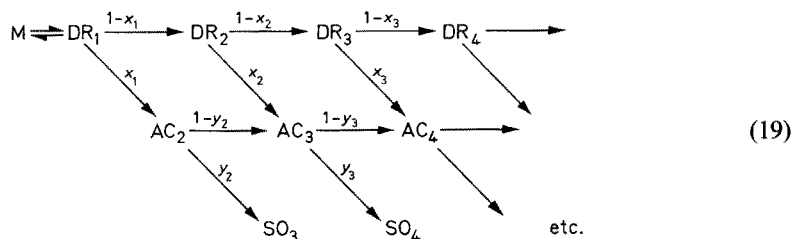
The concentration of the excited intermediates is proportional to the absorbed light intensity. In the case of indirect excitation via energy transfer ($M^* + M' + \text{RO} \rightarrow M + M'^* + \text{RO} \rightarrow M + M' + \text{RO}^*$) it is proportional to the concentration of the excited monomer molecules $[M^*]$.

The observed time evolution and the decay of the photoproduct absorptions by photochemical and/or thermal reactions in the TS diacetylene crystals are described quantitatively by Eqs. (15) to (18). This has been demonstrated by Hersel⁵⁸⁾, Neumann^{62, 63)}, and Niederwald^{51, 52)}. Some examples of calculated curves are shown in Figs. 5, 10, and 12.

Thermal chain termination reactions have not been observed in the spectra of the short chain intermediates with $n \lesssim 10$. Therefore much longer final polymer molecules are expected in the thermal reactions. From the analysis of our optical absorption spectra⁶⁸⁾ an average chain length of $\bar{n} \approx 150$ is estimated for the final polymer molecules obtained after thermal addition reactions.

4.2 Chain Lengths Distribution

As we have seen above there are certain probabilities x_n in all low temperature photo-addition reaction steps that the first termination reaction will occur, i.e. the transformation of the diradical intermediates to the asymmetric carbene intermediates ($\text{DR}_n \rightarrow \text{AC}_{n+1}$). The second termination reactions, in which finally the stable oligomers are produced from the AC intermediates ($\text{AC}_n \rightarrow \text{SO}_{n+1}$) may be characterized by the probabilities y_n . Therefore, a simplified reaction scheme is given by:



The reactions within the DR and AC series are given by the probabilities $(1 - x_n)$ and $(1 - y_n)$, respectively. Because the chemical character of the intermediates is not a function of chain length the probabilities are assumed to be independent of n , therefore $x_n = x$ and $y_n = y$. In this model, due to the branching of the photochemical reactions, the intermediates are not expected to become infinitely long. Thus, a distribution of chain lengths will be obtained for the DR intermediates, different from those of the AC and SO intermediates. The different chain length distributions — obtained under stationary conditions — are dependent on the probabilities x and y and on the different rate constants k_n^{DR} and k_n^{AC} . They follow from the kinetic equations

$$\begin{aligned} d[\text{DR}_n]/dt &= (1 - x) k_{n-1}^{\text{DR}} [\text{DR}_{n-1}] [\text{M}'^*] \\ &\quad - k_n^{\text{DR}} [\text{DR}_n] [\text{M}'^*] = 0, \quad n \geq 2, \\ d[\text{AC}_n]/dt &= (1 - y) k_{n-1}^{\text{AC}} [\text{AC}_{n-1}] [\text{M}'^*] \\ &\quad + x k_{n-1}^{\text{DR}} [\text{DR}_{n-1}] [\text{M}'^*] \\ &\quad - k_n^{\text{AC}} [\text{AC}_n] [\text{M}'^*] = 0, \quad n \geq 3, \\ d[\text{SO}_n]/dt &= + y k_{n-1}^{\text{AC}} [\text{AC}_{n-1}] [\text{M}'^*] > 0, \quad n \geq 3. \end{aligned} \quad (20)$$

Stationary conditions are obtained after prolonged UV-irradiation times. In order to obtain a better understanding we will concentrate on the simplest situation characterized by $k_n^{\text{DR}} = k_n^{\text{AC}} = k$. If we refer to the first stable diradical DR_2 (denoted by A in the optical spectra and by I in the ESR spectra), we obtain the following distribution described by:

$$\begin{aligned} [\text{DR}_n] &= (1 - x)^{n-2} [\text{DR}_2], \quad n \geq 2, \\ [\text{AC}_n] &= (1 - y) [\text{AC}_{n-1}] + x(1 - x)^{n-3} [\text{DR}_2] \end{aligned}$$

with

$$\begin{aligned} [\text{AC}_2] &= \frac{x[\text{DR}_2]}{1 - x}, \quad n \geq 3, \\ [\text{SO}_n] &= y[\text{AC}_{n-1}] k \int_0^t [\text{M}'^*] dt. \end{aligned} \quad (21)$$

In contrast to the DR and AC intermediates the concentration of the SO molecules is dependent on the UV-irradiation time. All concentrations are independent of the UV-intensity.

Figure 23 shows the stationary distribution of the DR- and AC-intermediates and of the SO molecules obtained with Eq. (21) for $x = 0.2$ and $y = 0.1$. The distribution of the DR and AC molecules has been normalized on the DR_2 concentration, representing the shortest DR intermediate, which are stable at low temperatures in contrast to the short-lived excited DR_1 molecules. The distribution function of the SO molecules has been normalized with $[\text{SO}_3] = 1$. The SO_3 molecules are the shortest stable oligomer molecules.

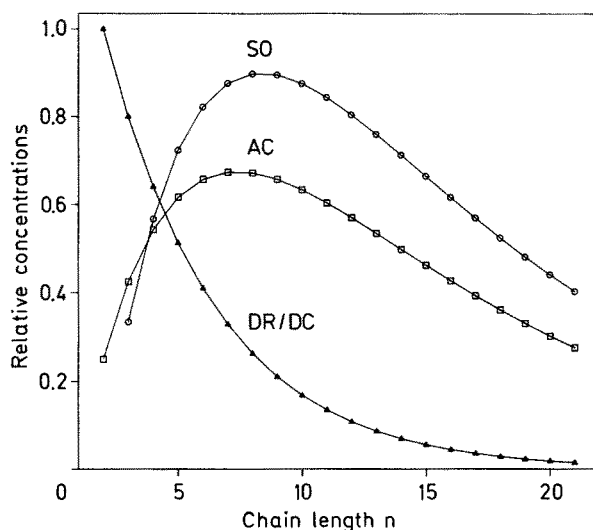


Fig. 23. Calculated chain length distribution in TS-6 during stationary UV-illumination using the probabilities $x_n = x = 0,2$ and $y_n = y = 0,1$

The distribution function of the DR intermediates is a simple exponential function. Therefore, the average chain length of the DR intermediates is simply $\bar{n}(\text{DR}) = 1 + 1/x$. The situation of the AC and SO molecules is more complex. The average chain length is $\bar{n}(\text{AC}) = 1 + 1/x + 1/y$ and $\bar{n}(\text{SO}) = \bar{n}(\text{AC}) + 1$. The distributions shown in Fig. 23 are only a rough approximation to the experimental observations; they clearly show the rapid decrease of the absorption intensities at longer chain length observed in the experiments of the low temperature photopolymerization process. A more detailed analysis has been given by Gross et al. ⁸⁵⁾

5 Primary Processes

5.1 Dimer Initiation

The energy level scheme of the monomer diacetylene TS-6 crystals is shown in Fig. 24. The positions of the excited singlet (S) and triplet states (T) of the diacetylene unit $-\text{C}\equiv\text{C}-\text{C}\equiv\text{C}-$ follow from the optical absorption [86] and emission spectra ⁸⁷⁾ of the pure monomer crystals. In most cases the UV excitation of the monomer crystal is performed in the extreme absorption edge of the $S_0 \rightarrow S_1$ absorption in order to obtain a very homogeneous distribution of reaction centers M^* throughout the crystal. The energy then is expected to relax very rapidly into the lowest excited triplet state $S_1 \rightarrow T_1$ via intersystem crossing and internal conversion processes. In TS-6 the lowest excited states of the substituents R lie above the corresponding excited singlet and triplet states of the diacetylene unit.

At low temperatures the polymerization process is only initiated by UV-, γ - or x-irradiation via excitation of the monomer molecules. However, in order to understand the relatively high quantum yield obtained in the bimolecular initiation reaction of Eq. (9) we have to consider a metastable long-lived excited state M^* , which represents

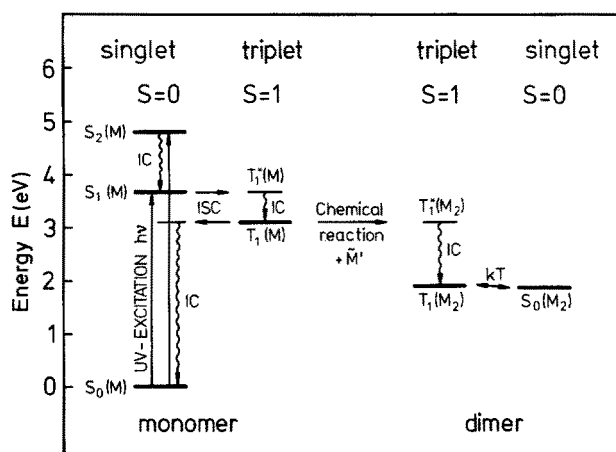
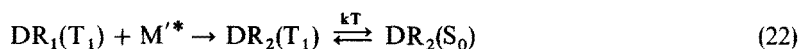


Fig. 24. Energy level diagram of the photophysical and photochemical primary processes of the low temperature photopolymerization reaction in diacetylene crystals. IC: Internal Conversion; ISC: Intersystem Crossing

the reaction center of the initiation reaction. The monomer diradical $T_1(M) = DR_1$ of Fig. 24 with the structure $R-\dot{C}=C=C=\dot{C}-R$ is a good approximation of the lowest excited $\pi\pi^*$ singlet and $\pi\pi^*$ triplet state of the diacetylene molecule in the *trans* configuration. The excitation energy of a monomer dicarbene DC_1 with the structure $R-\dot{C}-C\equiv C-\dot{C}-R$ is very high in energy (due to the additional loss of a π -bond) and is, therefore, not considered in the discussion. Even upon direct excitation into the dicarbene state the molecule is expected to relax very rapidly into the lowest excited T_1 state.

The most probable photochemical primary process of the polymerization reaction is shown in the energy level diagram of Fig. 24. In the photoinitiation reaction an excited adjacent monomer molecule M'^* is added to the reaction center, best represented by the metastable triplet DR_1 monomer molecule. Owing to the spin conservation rules, we conclude that an excited *triplet* dimer-diradical DR_2 is formed in the chemical reaction. We may, therefore, formulate the reaction as follows:



The triplet dimer diradical $DR_2(T_1)$ finally will relax into thermal equilibrium (kT) with its singlet ground state $DR_2(S_0)$. As we have seen from the ESR spectra (see Fig. 10) the energy separation between the singlet and triplet diradical states is very low and thermally activated transitions occur even at low temperatures. Furthermore the ESR spectra have revealed an admixture of about 10% carbene character with the diradical intermediates. This carbene character may be important in determining the probability x of the side reactions (see Eq. (19)) for the $DR \rightarrow AC$ chain termination reaction. It surely is not, however, the only essential factor, otherwise there should be no difference in the optical and thermal termination reaction steps. Up to now a direct observation of the metastable triplet state $T_1(M)$ has been possible only in two specific crystals^{87,88}, where the polymerization reactions are very weak.

The dimer initiation is a multistep process with two essential steps, the creation of the reaction center "DR₁" with reactive electrons and the addition of an excited adjacent molecule M^{*}. As we know from the thermal addition reaction steps at low temperatures the nature of the "second" excitation in the bimolecular reaction must be extremely low in energy and, therefore, electronic excitations may be excluded. On the other hand molecular motions are likely to be more important in the dimer formation process. Therefore we have to inspect the topochemistry of the reaction. The most probable mechanism of the dimer formation is shown in Fig. 25. In the first step (1) (only by optical excitation) the metastable reaction center is generated. In the second step (2) the motion required in the reaction is performed by librational excitation of the adjacent molecules. This librational excitation may be thermally activated and therefore is present in the crystals at elevated temperatures only. At low temperatures (T < 80 K) this librational excitation is generated only by absorption of photons with subsequent radiationless relaxation processes, producing phonons and librons. A detailed analysis of the dimer initiation process has been given by Neumann et al.⁸⁹⁾

The low activation energy of the thermal addition polymerization reaction confirms the necessity of a (librational) motion of the molecules in the initiation process. The first addition process differs from all the following addition processes by the metastable monomer diradical structure, which — in contrast to the DR_n, AC_n, and DC_n structures with n > 2 — has a limited life-time given by the phosphorescence decay of the monomer triplet state. Therefore, the librational excitation must be performed during the life-time of the monomer reaction centre. In the case of the low temperature photopolymerization reaction the librational excitation has to be prepared optically via the decay of the electronic excitation. This is in contrast to the photopolymerization reaction at high temperatures, where numerous molecular motions are thermally and stationary present in the crystals. Due to this difference two photons (2hν) are required in every dimer initiation process at low temperatures and only one photon (hν + kT) is required at high temperatures. The two paths of the photoinitiation reaction are illustrated below by the arrows in Fig. 26. The respective pair states are characterized by M^{*}M^{*} and M^{*}M' as discussed below.

In recent experiments the photopolymerization process has been initiated with visible light. Sensibilization of the photopolymerization reaction is possible in diacetylene crystals by introduction of energetically low lying absorptions of the substituents via formation of mixed crystals or by doping with dye molecules⁹⁰⁾. Although the detailed mechanism of the sensibilization is not clear, the experiments clearly demonstrate the importance of lowlying electronic states in the polymerization reaction.

5.2 Stability and Reactivity

In the discussion of the chain initiation and chain propagation reactions we need to consider the binding energies of the different DR, AC, DC intermediates and SO oligomer molecules. In first order they are obtained by simply summing up the energies of their π- and σ-bonds. From energetic considerations further informations concerning the paths of the individual polymerization reaction steps can be obtained.

In the DR_2 formation process two monomer molecules are connected by a single σ -bond yielding an energy of 3.6 eV. Simultaneously two monomer π -bonds with an energy of $2 \times 2.7 \text{ eV} = 5.4 \text{ eV}$ are disrupted. Consequently the net energy loss in the dimer DR_2 formation process amounts to $E(DR_2) = 1.8 \text{ eV}$.

In the DC_2 formation process two monomer molecules are connected by a double bond, yielding the energy of a $(\sigma + \pi)$ -bond. Simultaneously four monomer π -bonds are lost in the reaction. Consequently, according to $(3\pi - 1\sigma)$ -bonds, the net energy loss in the dimer DC_2 formation process amounts to $E(DC_2) = 4.5 \text{ eV}$. Due to this high energy no dimer dicarbenes are observed!

In the AC_2 formation process via a DC_2 excited state and simultaneous intramolecular insertion reaction following Eq. (8b) first the energy of the DC_2 formation is required. However, in the subsequent insertion reaction the energy of a π -bond is gained. Therefore the net energy amount is $E(AC_2\text{-intramol. insertion}) = (DC_2) - E(\pi) = 4.5 \text{ eV} - 2.7 \text{ eV} = 1.8 \text{ eV}$.

The AC_1 formation seems more probable than the AC_2 formation in an intramolecular insertion reaction. In this situation a DC_1 excited state is required, which reacts to the AC_1 state. The net energy amount of this reaction therefore is $E(AC_1\text{-intramol. insertion}) = E(DC_1) - E(\pi) = (2 \cdot 2.7 - 2.7) \text{ eV} = 2.7 \text{ eV}$.

In the AC_2 formation process, by an intermolecular CH_2 insertion reaction (8a) a σ -bond is formed upon disruption of two π -bonds. Therefore as with the DR_2 molecules the net energy loss amounts to $E(AC_2\text{-intermol. insertion}) = 1.8 \text{ eV}$. Upon formation of a pseudocyclopropene structure (7) three π -bonds are disrupted and two distorted σ -bonds (τ -bonds) with about 5 eV^{91} are formed. In this case the net energy loss amounts to $E(AC_2\text{-pseudocyclopropen}) \cong 3 \text{ eV}$.

In the bimolecular UV-photoinitiation reaction, due to the high energy of the monomer singlet excitation, an energy of $2 \times 4 \text{ eV}$ is available. According to the procedure described above, however, only one reaction centre is necessary, which has been interpreted as being the diradical monomer triplet state with an energy of about 3 eV. Compared to this value the librational excitation energy is negligibly small. With this energy of 3 eV only the DR- and AC-dimer but not the DC-dimer reactions are possible as observed experimentally.

In the chain propagation reaction a π -bond is changed into a σ -bond by addition of an adjacent monomer molecule to the intermediates. In this way in every reaction step about 0.9 eV are released. The resulting energy level scheme of the polymerization reaction is shown in Fig. 26. It represents the energetic positions of the resulting DR or AC intermediates characterized by the general notation M_n and the transient pair states $M_n M'^*$ and $M_n \bar{M}'$. The addition reaction steps may be induced optically ($h\nu$) or thermally (kT). In both cases, according to our reaction model of Fig. 25, the reaction is presumed to pass the librational excitation \bar{M}' of the adjacent molecules via the relaxation step $M'^* \rightarrow \bar{M}'$. The small activation energies of the individual addition reaction steps at short chain lengths characterize the addition reaction, in which no further electrical excitation is required due to the presence of reactive radical or carbene chain ends of the DR, AC and DC intermediates.

In the thermal addition reaction a structural change from the butatriene to the acetylene chain structure is observed at $n = 6$ in the ESR spectra of the short intermediates. Since the ESR is sensitive only to unpaired electrons with $S \neq 0$ the butatriene-to-acetylene transformation is observed only in the thermally excited DR

and DC states and not in their corresponding ground states. The low activation energies, however, suggest an almost identical chain structure in the $S = 0$, $S = 1$ or $S = 2$ states. Moreover from the optical spectra, which are sensitive to the chain structure only, it is not possible to distinguish between states of different multiplicity. By simply counting the σ - and π -bonds the DR intermediates should be more stable than the DC intermediates by an amount of 2.7 eV, corresponding to the additional π -bond. This energy difference obviously is compensated by a slightly higher stability

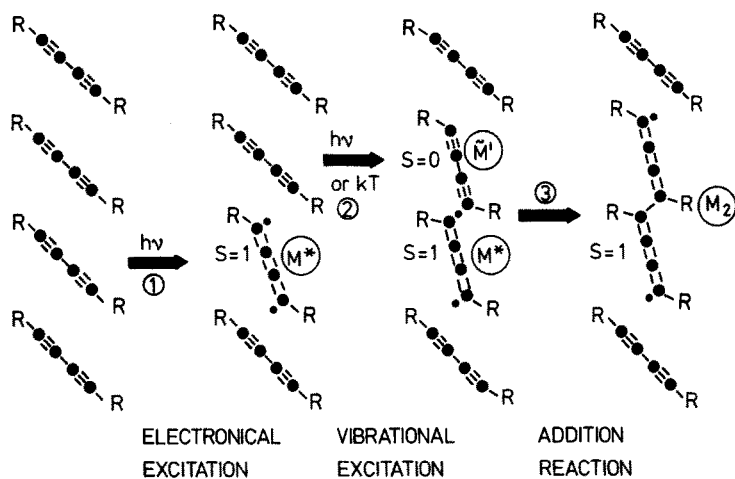


Fig. 25. Reaction scheme of the dimer initiation reaction. (1) Formation of the metastable monomer diradical M^* ; (2) Distortion of the adjacent monomer molecule M' ; (3) Formation of the diradical dimer molecule M_2 by 1,4 addition

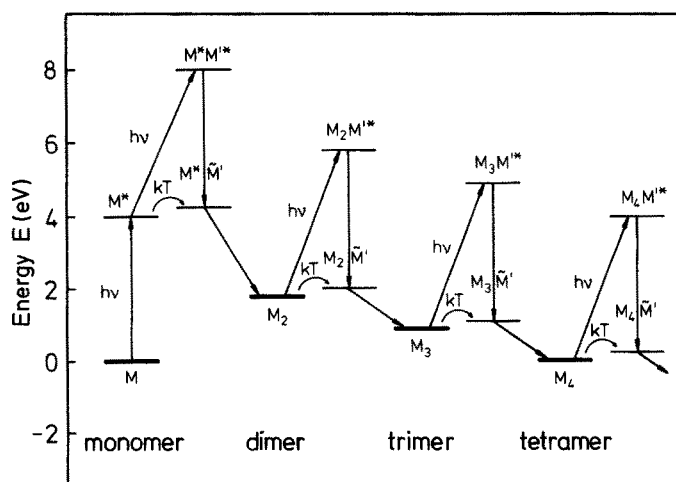


Fig. 26. Energy level scheme representing the initial steps of the polymerization reaction. The two paths of the optical ($h\nu$) and thermal (kT) addition reaction are characterized by the arrows

of the acetylene units $\text{—RC—C}\equiv\text{C—CR—}$ as compared to the butatriene units —RC=C=C=CR— , which have the same total number of σ - and π -bonds. An energy difference of about 0.4 eV per unit easily could explain the observed structural change at about $n = 6$. This butatriene-to-acetylene transformation has been observed also in the TS-12 and TCDU diacetylene crystals⁹²⁻⁹⁴⁾ at about the hexamer unit.

The binding energies, gained in the termination reaction $\text{DC} \rightarrow \text{AC}$ and $\text{AC} \rightarrow \text{SO}$ by saturation of the carbene ends, are identical. However the insertion reactions (8) with an energy gain of 3.6 eV are energetically favoured as compared to the pseudocyclopropene reaction with only 2.3 eV. In the $\text{DR} \rightarrow \text{AC}$ termination reaction the radical electron pair is maintained and therefore only a low change in the stability is expected. However, energy is gained by the structural butatriene-to-acetylene transformation. Again the insertion reactions (with $n \cdot 0.4 \text{ eV} + 0.9 \text{ eV}$) are energetically favoured as compared to the pseudocyclopropene reaction (with $n \cdot 0.4 \text{ eV} - 0.4 \text{ eV}$). The optically induced chain terminations are very efficient. However, thermal chain termination reactions have not been observed with the short chain intermediates with $n \lesssim 10$, which may be resolved either in the optical or ESR absorption spectra. Consequently, in contrast to the pure photopolymerization reaction at low temperatures much longer polymer chains with $n \approx 150$ ⁶⁸⁾ are obtained in the high temperature photopolymerization reaction, where — after photoinitiation — subsequent thermal addition polymerization reactions are very effective.

6 Conclusions

From the experimental results and conclusions drawn from the investigations of the TS-6 model system we may be able to derive general characteristics of the polymerization reaction in diacetylene crystals. This is due to the fact, that — as a rule — the diradical, carbene and dicarbene intermediates are not directly dependent on the structure and chemical properties of the substituents. For instance, in BPG⁸⁸⁾ and TCDU⁴⁷⁾ crystals carbene states (located at the ends of long oligomer molecules) have been also detected in the ESR spectra, which are very similar to those in TS-6. The similarity of the optical absorption spectra of the short chain intermediates is demonstrated in Fig. 8 which shows the same diradical series A, B, C, ... in TCDU, TCDA and TS-12²⁶⁾ as observed in the TS-6 crystals even at almost the same energetic positions. Differences in the polymerization reactions in the differently substituted diacetylene crystals essentially arise from the specific molecular arrangements, resulting in specific changes of the distances and orientations of the reactive centres of the individual molecules. Therefore, the distinct reactivities of the different diacetylene crystals are predetermined by their distinct topochemistry of essentially the dimer initiation reaction, which dominates the overall quantum yield of the polymerization reaction.

Owing to the bimolecularity of the initiation reaction the quantum yield of the dimer molecules (M_2/N_{abs}) is proportional to the absorbed light quanta N_{abs} and to the ratio k_1/k_0 , characterizing the competition of the chemical dimer initiation process (k_1) with the deactivation processes (k_0) of the monomer excitation. A comparison of the dimer A absorption intensities of different diacetylene crystals shows that the ratio k_1/k_0 is about a factor of 10^2 to 10^3 larger in the TS-6 crystals than in

the TS-12, TCDU or BPG crystals. The high photoreactivity of our model system TS-6 therefore, gives good experimental conditions for a detailed analysis of all the different reaction intermediates. Nevertheless, the quantum yield of about 10^{-2} (that is 100 photons per reaction step⁵⁶⁾) in TS-6 crystals is low as compared to the photochemical processes using silver halides and, therefore, at the moment is only of minor importance for technical applications.

In this article it has been shown, that the low temperature photopolymerization reaction of diacetylene crystals is a highly complex reaction with a manifold of different reaction intermediates. Moreover, the diacetylene crystals represent a class of material which play a unique role within the usual polymerization reactions conventionally performed in the fluid phase. The spectroscopic interest of this contribution has been focussed mainly on the electronic properties of the different intermediates, such as butatriene or acetylene chain structure, diradical or carbene electron spin distributions and spin multiplicities. The elementary chemical reactions within all the individual steps of the polymerization reaction have been successfully investigated by the methods of solid state spectroscopy. Moreover we have been able to analyze the physical and chemical primary and secondary processes of the photochemical and thermal polymerization reaction in diacetylene crystals. This success has been largely due to the stability of the intermediates at low temperatures and to the high informational yield of optical and ESR spectroscopy in crystalline systems.

Acknowledgements: The work has been supported by the Deutsche Forschungsgemeinschaft and by the Stiftung Volkswagenwerk.

Some investigations have been performed in collaboration with chemists (Prof. G. Wegner, Freiburg) and physicists (Prof. M. Schwoerer, Bayreuth and Prof. H. C. Wolf, Stuttgart). Helpful discussions with C. Bloor, D. Batchelder, H. Gross, W. Neumann, D. Siegel, and K. Ulrich are gratefully acknowledged.

7 References

1. Wunderlich, B.: *Macromolecular Physics*, Vol. 2, N.Y., Academic Press, 1976
2. Uhlmann, D. R. and Kolbeck, A. G.: *Sci. Am.* 233, 96 (1975)
3. Keller, A.: *Phil. Mag.* 2, 1171 (1957)
4. Geil, P. H.: *Polymer Single Crystals*, Interscience, New York 1963
5. Wegner, G.: *Z. Naturforschung* 24b, 824 (1969)
6. Wegner, G.: *Die Makromolekulare Chemie* 134, 219 (1970) and 154, 35 (1972)
7. Wegner, G.: *Chimia* 28, 475 (1974)
8. Wegner, G.: in *Molecular Metals* (ed. by Hatfield, W. E.), Plenum Press, N.Y. 209 (1979)
9. Wegner, G.: in *Chemistry and Physics of One-Dimensional Metals* (ed. by Keller, H. J.), Plenum Press, N.Y. 297 (1977)
10. Baughman, R. H.: *J. Appl. Phys.* 43, 4362 (1972)
11. Baughman, R. H.: *J. Polym. Sci., Polym. Phys. Ed.* 12, 1511 (1974)
12. Baughman, R. H. and Yee, K. C.: *J. Polym. Sci., Polym. Chem. Ed.* 12, 2467 (1974)
13. Baughman, R. H. and Chance, R. R.: in *Synthesis and Properties of Low-Dimensional Materials* (ed. by Miller, J. S. and Epstein, A.), Acad. Science, N.Y. 705, (1978)
14. Bloor, D.: in *Developments in Crystalline Polymers* (ed. by Bassett, D. C.), Appl. Sci. Publ. London, 1982 in press
15. Wunderlich, B.: *Adv. Polym. Sci.* 5, 566 (1968)
16. Geserich, H. P. and Pintschovis, L.: *Festkörperprobleme* 16, 65 (1976); Street, G. B. and Greene, R. L.: *IBM Res. Development* 21, 99 (1977)

17. Lochner, K., Reimer, B., and Bässler, H.: *Chem. Phys. Lett.* **41**, 388 (1976); *Phys. Stat. Sol. (b)* **76**, 533 (1976)
18. Bloor, D. and Preston, F. H.: *Phys. Stat. Sol. (a)* **37**, 427 (1976)
19. Reimer, B. and Bässler, H.: *Chem. Phys. Lett.* **43**, 81 (1976); *Phys. Stat. Sol. (a)* **32**, 435 (1975); **(b)** **85**, 145 (1978)
20. Wilson, E. G.: *J. Phys. C* **8**, 727 (1980); **13**, 2885 (1980)
21. Siddiqui, A. S.: *J. Phys. C* **13**, 2147 (1980)
22. Greene, R. L., Street, G. B., and Stuter, L. J.: *Phys. Rev. Lett.* **34**, 577 (1975)
23. Baughman, R. H., Chance, R. R., and Cohen, M. J.: *J. Chem. Phys.* **64**, 1869 (1976); Baughman, R. H., Chance, R. R.: *J. Polym. Sci., Polym. Phys. Ed.* **14**, 2019 (1976)
24. Leyrer, R. J., Wegner, G., and Wettling, W.: *Ber. Bunsenges. Phys. Chem.* **82**, 697 (1978)
25. Mondong, R. and Bässler, H.: *Chem. Phys. Lett.* **78**, 371 (1981)
26. Wenz, G. and Wegner, G.: *Makromol. Chem. Rapid. Comm.*, to be published; Siegel, D., Sixl, H., Enkelmann, V., and Wenz, G.: *Chem. Phys.* **72**, 201 (1982)
27. Bloor, D., Koski, L., Stevens, G. C., Preston, F. H., Ando, D. J.: *J. Mat. Sci.* **10**, 1678 (1975)
28. Niederwald, H., Richter, K.-H., Güttler, W., and Schwoerer, M.: *Laser Chemistry* (1983) to be published
29. Kohlschütter, H. W.: *Z. anorg. Chem.* **105**, 121 (1918)
30. Thomas, J. M.: *Phil. Trans. Roy. Soc. A* **277**, 251 (1974)
31. Cohen, M. D.: *Angew. Chem.* **87**, 439 (1975)
32. Meyer, W., Lieser, G., and Wegner, G.: *J. Polymer Sci. Polym. Phys. Ed.* **16**, 1365 (1978)
33. Nakanishi, H., Hasegawa, M., and Sasada, Y.: *J. Polymer Sci. A* **1**, 7, 735 (1969), and **A 2**, **10**, 1573 (1972)
34. Kobelt, D. and Paulus, E. F.: *Acta crystallogr. B*, **30**, 232 (1974)
35. Enkelmann, V. and Wegner, G.: *Makromol. Chem.* **178**, 635 (1977)
36. Enkelmann, V.: *Acta Cryst. B* **33**, 2842 (1977)
37. Enkelmann, V. and Wegner, G.: *Angew. Chem.* **89**, 432 (1977)
38. Enkelmann, V., Leyrer, R. J., and Wegner, G.: *Makromol. Chem.* **180**, 1787 (1979)
39. Bloor, D.: *Europhys. News* **8**, 1 (1977)
40. Bloor, D., Preston, F. H., and Ando, J.: *Chem. Phys. Lett.* **38**, 33 (1976)
41. Reimer, B., Bässler, H., Hesse, J., and Weiser, G.: *Phys. Stat. Sol. (b)* **73**, 709 (1976)
42. Bloor, D., Ando, D. J., Preston, F. H., and Batchelder, D. N.: in *Structural Studies of Macromolecules by Spectroscopic Methods* (ed. by K. J. Ivin), Wiley (1976) 91
43. Bloor, D. and Preston, F. H.: *Phys. Stat. Sol. (a)* **39**, 607 (1977); **40**, 279 (1977)
44. Hersel, W.: *Thesis Univers. Stuttgart* (1981)
45. Kuhn, H.: *J. Chem. Phys.* **17**, 1198 (1949)
46. Exarhos, G. J., Risen, jr., W. M., and Baughman, R. H.: *J. Am. Chem. Soc.* **98**, 481 (1976)
47. Gross, H., Sixl, H., Kröhnke, C., and Enkelmann, V.: *Chem. Phys.* **45**, 15 (1980)
48. Bloor, D., Ando, D. J., Preston, F. H., and Stevens, G. C.: *Chem. Phys. Lett.* **24**, 407 (1974)
49. Stevens, G. C. and Bloor, D.: *J. Polym. Sci. Polym. Phys. Ed.* **13**, 2411 (1975); *Chem. Phys. Lett.* **40**, 37 (1976)
50. Eichele, H., Schwoerer, M., Huber, R., and Bloor, D.: *Chem. Phys. Lett.* **42**, 342 (1976)
51. Niederwald, H., Eichele, H., and Schwoerer, M.: *Chem. Phys. Lett.* **72**, 242 (1980)
52. Niederwald, H. and Schwoerer, M.: *Z. Naturforsch.* **38a**, 749 (1983); Niederwald, H.: *Thesis, Univers., Bayreuth* (1982)
53. Hori, Y. and Kispert, L. D.: *J. Chem. Phys.* **69**, 3826 (1978)
54. Hori, Y. and Kispert, L. D.: *J. Am. Chem. Soc.* **101**, 3173 (1979)
55. Bubeck, C., Sixl, H., and Wolf, H. C.: *Chem. Phys.* **32**, 231 (1978)
56. Bubeck, C., Neumann, W., and Sixl, H.: *Chem. Phys.* **48**, 269 (1980)
57. Sixl, H., Hersel, W., and Wolf, H. C.: *Chem. Phys. Lett.* **53**, 39 (1978)
58. Hersel, W., Sixl, H., and Wegner, G.: *ibid.* **73**, 28 (1980)
59. Wegner, G.: *Pure Appl. Chem.* **49**, 443 (1977)
60. Wegner, G., Arndt, G., Graf, H.-J., and Steinbach, M.: in *Reactivity of Solids* (ed. by Wood, J., Lindqvist, O., Helgesson, C., and Vannerberg, N.-G.), Plenum Press 487 (1977)
61. Chance, R. R. and Patel, G. N.: *J. Polym. Sci. Polym. Phys. Ed.* **16**, 859 (1978)
62. Neumann, W. and Sixl, H.: *Chem. Phys.* **50**, 273 (1980)
63. Neumann, W. and Sixl, H.: *ibid.* **58**, 303 (1981)

64. Huber, R. and Schwoerer, M.: *Chem. Phys. Lett.* 72, 10 (1980)
65. Bubeck, C., Hersel, W., Sixl, H., and Waldmann, J.: *Chem. Phys.* 51, 1 (1980)
66. Huber, R. A., Schwoerer, M., Benk, H., and Sixl, H.: *Chem. Phys. Lett.* 78, 416 (1981)
67. Hartl, W. and Schwoerer, M.: *Chem. Phys.* 69, 443 (1982)
68. Gross, H. and Sixl, H.: *Mol. Cryst. Liq. Cryst.* 93, 261 (1983); Gross, H.: Thesis, Univers. Stuttgart (1983)
69. Gross, H. and Sixl, H.: *Chem. Phys. Lett.* 91, 262 (1982)
70. Brédas, J. L., Chance, R. R., Silbey, R., Nicolas, G., and Durand, Ph.: *J. Chem. Phys.* 75, 255 (1981)
71. Hädicke, E., Mez, E. C., Krauch, C. H., Wegner, G., and Kaiser, J.: *Angew. Chem.* 83, 253 (1971)
72. Huber, R., Schwoerer, M., Bubeck, C., and Sixl, H.: *Chem. Phys. Lett.* 53, 35 (1978)
73. Bernheim, R. A., Kempf, R. J., Gramas, J. V., and Skell, P. S.: *J. Chem. Phys.* 43, 196 (1965)
74. Bernheim, R. A., Bernhard, H. W., Wang, P. S., Wood, L. S., and Skell, P. S.: *J. Chem. Phys.* 53, 1280 (1970)
75. Hutchison, jr., C. A. and Kohler, B. E.: *J. Chem. Phys.* 51, 3327 (1969)
76. Murray, R. W. and Trozzolo, A. M.: *J. Org. Chem.* 29, 1268 (1964)
77. Bubeck, C.: Thesis Univers. Stuttgart (1979)
78. Kirmse, W.: *Carbene Chemistry*, Academic Press, N.Y. (1971)
79. Jones, J. J. M.: *Sci. Am.* 2, 101 (1976)
80. Benk, H. and Sixl, H.: *Mol. Phys.* 42, 779 (1981)
81. Schwoerer, M., Huber, R. A., and Hartl, W.: *Chem. Phys.* 55, 97 (1981)
82. Kollmar, C., Sixl, H., Benk, H., Denner, V., and Mahler, G.: *Chem. Phys. Lett.* 87, 266 (1982)
83. Neumann, W.: Thesis, Univers. Stuttgart (1983)
84. McGhie, A. R., Kalayanaraman, P. S., and Garito, A. F.: *J. Polym. Sci. Polym. Lett. Ed.* 16, 335 (1978)
85. Gross, H., Neumann, W., and Sixl, H.: *Laser Chemistry* (1983) in press
86. Kawaoka, K.: *Chem. Phys. Lett.* 37, 561 (1976); Hardwick, J. L. and Ramsay, D. A.: *Chem. Phys. Lett.* 48, 399 (1977)
87. Bertault, M., Fave, J. L., and Schott, M.: *Chem. Phys. Lett.* 62, 161 (1979)
88. Bubeck, C., Sixl, H., Bloor, D., and Wegner, G.: *Chem. Phys. Lett.* 63, 574 (1979)
89. Gross, H., Neumann, W., and Sixl, H.: *Chem. Phys. Lett.* 92, 584 (1983)
90. Tieke, B. and Wegner, G.: *Makromol. Chem.* 179, 2573 (1978); Enkelmann, V., Tieke, B., Knapp, H., Lieser, G., and Wegner, G.: *Ber. Bunsenges. Phys. Chem.* 82, 876 (1978); Braunschweig, F. and Bässler, H.: *ibid.* 84, 177 (1980); Bubeck, C., Tieke, B., and Wegner, G.: *ibid.* to be published
91. Lathan, W. A.: *Structures and Stabilities of Three Membered Rings in Topics Curr. Chem.*, Vol. 40, 1 (1973), Springer

H.-J. Cantow (Editor)

Received July 26, 1983